

## A Convective Model for the Weddell Polynya<sup>1</sup>

DOUGLAS G. MARTINSON

*Lamont-Doherty Geological Observatory and Department of Geological Sciences,  
Columbia University, Palisades, NY 10964*

PETER D. KILLWORTH

*Department of Applied Mathematics and Theoretical Physics, University of Cambridge, Cambridge, England*

ARNOLD L. GORDON

*Lamont-Doherty Geological Observatory and Department of Geological Sciences,  
Columbia University, Palisades, NY 10964*

(Manuscript received 9 June 1980, in final form 12 January 1981)

### ABSTRACT

Mechanisms are considered which may induce the large (over  $10^5$  km<sup>2</sup>) area of open water, or polynya, which frequently occurs within the Weddell Sea winter sea-ice. We propose that when surface cooling and ice formation decrease the temperature and increase the salinity of the surface water (the latter by salt rejection during ice formation) in a preconditioned area, static instability with intense vertical mixing can occur. The upwelled warm, salty deep water can then supply enough heat to melt the ice, or prohibit its formation, even in the middle of winter.

A simple two-level model is derived to test this theory and is found to agree well with observations. The process is found to be irregular due to different times of ice onset from one year to the next, and to a lesser extent from variations in surface heating and cooling. Further, it is shown that unless the freshwater input exactly balances the increased salinity from the overturn each year, the system will either gain or lose salt yearly and eventually stabilize permanently (i.e., attain a steady-state condition).

The model is insensitive to short term stochastic variations in surface heat flux or freshwater input rates, but is somewhat sensitive to longer scale variations in the net freshwater input and also to the depth of the pycnocline (i.e., preconditioning). It is suggested that upwelling may raise the pycnocline until convection can occur and the polynya form. The preconditioned area then advects westward with the mean flow. Permanent stability finally is attained but the preconditioned area is advected into the western boundary current of the Weddell subpolar gyre and destroyed. Prior to destruction, topographical features may quantitatively affect both the movement and occurrence of the polynya.

Regardless of the preconditioning mechanism, if overturning is responsible for the polynya, this would contribute a minimum of  $10^6$  m<sup>3</sup> s<sup>-1</sup> to the total deep water formation, and constitute the largest area of deep open-ocean convection yet discovered.

### 1. Introduction

A remarkable feature of the winter sea-ice distribution in the vicinity of the Weddell Sea is a large, irregularly appearing patch of open water. This open water, or polynya, appears in the middle of an otherwise all ice-covered region. Scattered sightings of the polynya in early spring, after it has opened to the northeast, have been reported for quite some time (Heap, 1964; Streten, 1973). It was not, however, until the sophistication of measurement techniques advanced sufficiently, so as to provide near continuous satellite coverage, that the polynya has been shown to exist in the winter and reliably documented.

The Weddell polynya, as we shall term it, is an anomalous phenomena, remarkable for a variety of reasons. First, it is comprised of an exceptionally large area of open water;  $\sim 0.3 \times 10^6$  km<sup>2</sup>. Second, unlike small nearshore polynyas frequently observed in polar and subpolar regions, this polynya occurs typically 800 km offshore. Third, the polynya occurs during intense winter cooling at a time when sea-ice cover should rapidly be growing thicker rather than disappearing. Finally, based on the short satellite record, the polynya appears to occur irregularly both temporally and spatially as seen in Fig. 1. Temporally the polynya was present for the entire winters of 1974–76; in 1973, 1977 and 1979 smaller, short-lived polynyas were observed, and in 1978 no polynya appeared. Spatially, in all cases the polynya occurs

<sup>1</sup> Lamont-Doherty Geological Observatory Contribution No. 3128.

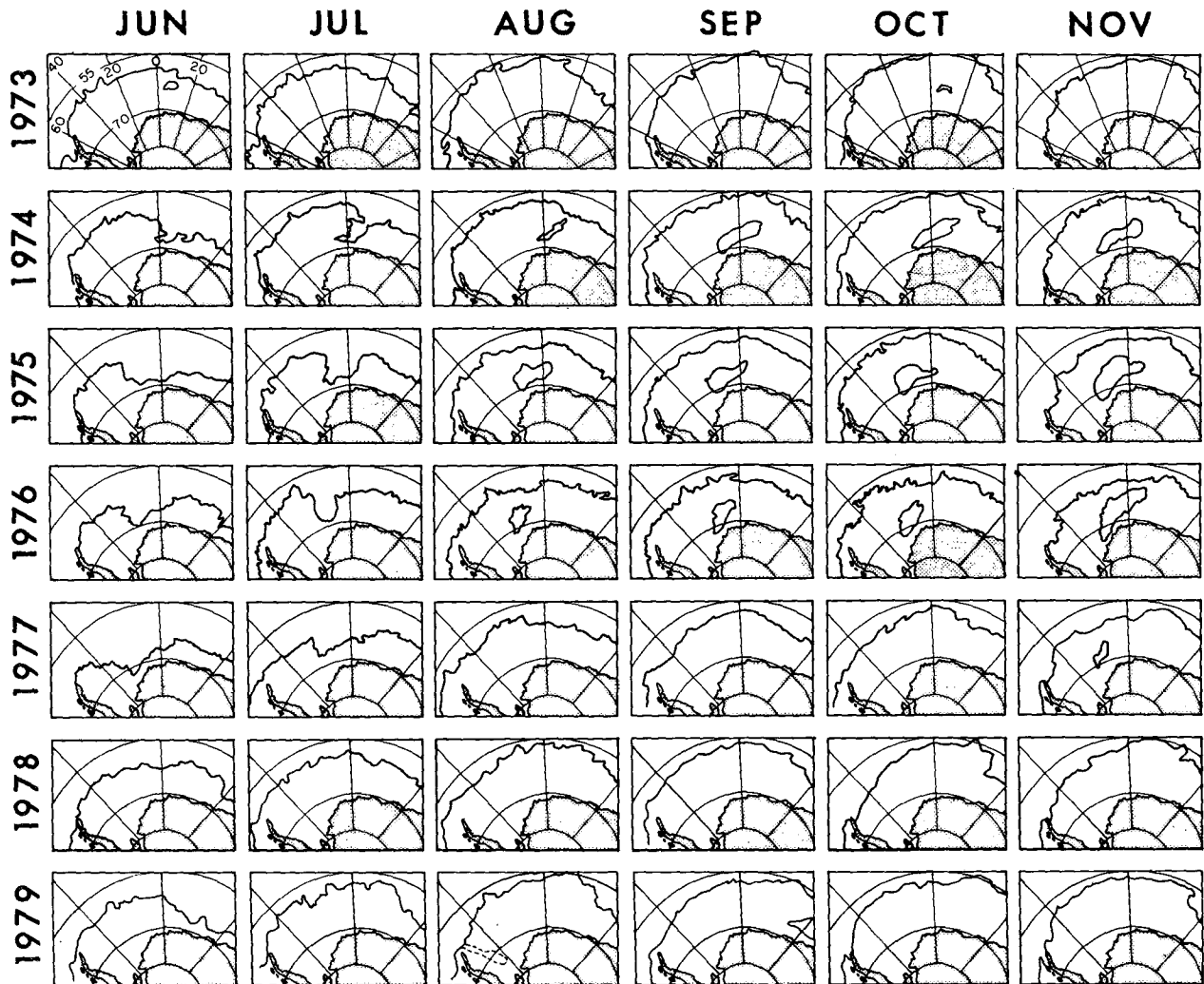


FIG. 1. Satellite record of ice distribution for June–November from 1973–79. Dashed polynya in August 1979 is reduction in ice, of up to 40% (from the Fleet Weather Weekly Ice Charts, 1973–1979).

at  $\sim 65^\circ\text{S}$  but its longitudinal position varies from as far west as  $20^\circ\text{W}$  to as far east as  $40^\circ\text{E}$ .

It is important to investigate the mechanisms producing this polynya apart from a basic interest in understanding an anomalous feature. This is because of its anticipated moderating effect on the local heat flux which substantially increases in areas of open water. In the presence of sea ice, the heat loss from ocean to atmosphere is strongly reduced; however, as little as 5% open water can increase the heat loss by 50% over its value with complete ice cover (Vowinkel and Orvig, 1970). Estimates presented later in this paper suggest that heat loss in late winter to spring is 8–10 times higher from open water than from ice covered water [it has been demonstrated by Moritz (1979) that in large leads or polynyas the air mass above the open water may become modified and reduce this heat flux by as much as 50%]. With the polynya occupying (conservatively) one tenth to

one eighth the area of the Weddell gyre, the heat loss in the gyre during winter can easily be increased 25–50% when the polynya is present. Conversely, in winters when the polynya is not present, the gyre must become warmer due to the ice insulation unless counteracted by decreased advection of heat from the north. Therefore, the theoretical as well as observational understanding of this anomalous phenomena clearly is necessary for the comprehension of the winter heat budget of the Weddell subpolar gyre.

This paper will address three major questions pertaining to the polynya:

- 1) Why does it occur?
- 2) Why does it occur where it does?
- 3) Why is its occurrence irregular?

The format of the paper is as follows: Section 2 contains various mechanisms for its formation; in Sections 3–5 a model of vertical heat exchange and

overturning is presented; Section 6 contains some properties of the model and a qualitative analysis; in Section 7 the data and model results are described; Section 8 contains a brief analysis of the effects of stochastic forcing and model sensitivity and the paper concludes with some speculations about the polynya.

## 2. Mechanisms for the polynya

### a. Divergent wind fields

The simplest mechanism which might be attributed to the formation of the polynya is the export of ice due to the divergent wind field. With this, the ice formed in wintertime is simply exported from its area of formation by wind-stress and frictional effects. This results in a latent heat polynya in which the sea-to-air heat flux is derived from the latent heat of fusion.

Although the mean wind field is certainly divergent, the area of maximum mean divergence is well north and east of the area in which the polynya is consistently formed. It would thus be expected that the mean wind field would yield polynyas in areas other than where they are observed. Furthermore, the rate of ice export required to maintain a near ice free condition in the polynya area would be of the order of meters per second. The standard rule of thumb for sea-ice drift today is one-fiftieth the wind speed [this is the approximate average of all the referenced values presented in Fig. 1 of James (1966, p. 37)]. To maintain these ice export rates therefore would require wind speeds averaging over  $50 \text{ m s}^{-1}$  (100 kt) which is clearly too large to be reasonable. In light of this discussion, we consider this mechanism to be unacceptable.

Another potential source of atmospheric divergence, however, lies in the response of the atmosphere to the polynya itself. The sea surface during a polynya is significantly warmer than areas of ice cover. Tropical observations of surface temperature anomalies suggest that this could produce a large low-pressure area over the polynya. If this were the case there would be ice export from the polynya area due to the induced atmospheric divergence. But, while this is likely to be a factor in the maintenance of the polynya, there are two objections to its being responsible for its formation. First, given the short atmospheric decay times and the frequent passages of energetic systems through the area it would seem difficult for the low-pressure area to survive coherently from one winter to another. Second, such a mechanism clearly cannot initiate a polynya as the polynya's existence is required to induce the mechanism to begin with.

### b. Upwelling of warm deep water

If the ice is not physically removed from the polynya area then it must instead be melted or pre-

vented from forming. To do this to  $3 \times 10^{11} \text{ m}^3$  of ice in the middle of the Antarctic winter obviously requires a strong source of heat. The heat is patently unavailable from the winter atmosphere and hence must be provided by the ocean. This is an attractive idea as an upward flux of oceanic heat does seem to be important in producing and maintaining the observed Weddell "chimney" (Gordon, 1978; Killworth, 1979).

The question then arises as to whether or not this heat can be created by a gradual upwelling. If this were the case the polynya would be expected to form at the center of the mean large-scale cyclonic Weddell gyre where upwelling is a maximum. This, though, is well north and east of the observed polynya area (Gordon *et al.*, 1977). Alternatively, anomalous Ekman pumping induced by the interaction of the polynya and atmosphere will certainly bring up warm deep water. This mechanism, however, suffers from the same problem about initialization as does its atmospheric counterpart previously discussed. But, unlike the atmospheric case, the area of upwelled water could be expected to remain roughly coherent from year to year (because the internal Rossby wave speeds are so slow at such latitudes). Thus anomalous Ekman pumping could be expected to have a role in the maintenance of the polynya.

### c. Convective processes

If the mean atmospheric and oceanic circulations are not responsible for the polynya's occurrence, then some more transient feature must be. Eddying and accompanying small-scale convection (cells of overturn  $\sim 4 \text{ km}$  across) does seem to occur in the Weddell subpolar gyre (Gordon, 1978; Killworth, 1979), but on scales far smaller than the polynya. This does suggest, however, that the predominant mechanism producing the polynya may be a vertical redistribution of heat with weak horizontal variation (strong horizontal variation would tend to occur in scales of the internal radius of deformation,  $\sim 20 \text{ km}$ ). This suggests an alternative theory which is put forth here. The theory is as follows.

A preconditioning is required to raise a large area of the pycnocline (at the moment the preconditioning mechanism is left unspecified). This then decreases the thickness of the surface level while making distinct an upper and lower water mass. During the winter the buoyancy above the pycnocline is strongly reduced both by heat losses to the atmosphere and ice, as well as by salt rejection during ice formation. Because of the thinness of the upper level above the raised pycnocline, the overall density here will increase rapidly until it becomes as dense as the lower level. At this density overturning will occur and the warm, salty deep water will mix with the cold, fresh surface water. The large volume of deep water will dominate the mixture resulting

in a warm, salty water mass which will melt the ice and form the polynya. A net freshwater input (e.g., excess precipitation over evaporation, continental runoff and ice import from the surrounding ice field) will then slowly decrease the salinity of the surface level which will in turn stabilize the system until the following winter.

Since the main oceanic motion is geostrophic, flow would tend to be around the area of overturning rather than into it so a purely vertical mixing is still approximately valid. Indeed, cross-frontal mixing concepts (Killworth, 1976) would suggest velocities into the overturning region of  $\sim 2 \times 10^{-4} \text{ m s}^{-1}$ . Even if this carried in water  $1^\circ\text{C}$  warmer or cooler than the overturning water, this would at most have a 5% effect on the heat budget. Additionally, the mean flow in the area is weak ( $\sim 0.01 \text{ m s}^{-1}$ ) so the polynya area should tend to remain roughly coherent from year to year. Hence we can consider the problem as being purely vertical with little loss of generality (the effects of horizontal advection can be included as a separate return to normal term in the heat equation as discussed in Section 3). Further, the mechanism tends to be self-sustaining; overturning in a polynya year serves to precondition the area for the following year (although not always successfully as will be shown). Finally, it is the only mechanism which might be expected to yield the observed coherency in the shape of the polynya throughout the season and from year to year (Carsey, 1980). Certainly, anomalous Ekman or wind field divergences would not be expected to produce such coherency.

### 3. A simple two-level model

To suggest that the above mechanism may be the dominant mechanism among those discussed needs some qualitative and quantitative testing. To this end we have created the following simple model.

As indicated, the system is justifiably simplified to a purely vertical one and is therefore modeled as being one-dimensional in the vertical. Also, for the purpose of modeling, the system has been further simplified to just two levels (*not* layers) of constant depth, each with a density uniform over the level. In other words the model is simplified to a two-level truncation of the Bryan (1969) finite-difference scheme. This is chosen not merely because a two-level representation resembles the stratification near the polynya area (this is seen in Fig. 2 in which the belt  $65^\circ\text{--}70^\circ\text{S}$ ,  $40^\circ\text{E--}40^\circ\text{W}$  has a decidedly two-level character), but to obtain a system which can be quantitatively analyzed. We do not think of the two-level structure therefore as an accurate representation of reality but as a means for studying some simplified physics.

Further, we have rejected such possibilities as a uniform lower level and a stratification varying line-

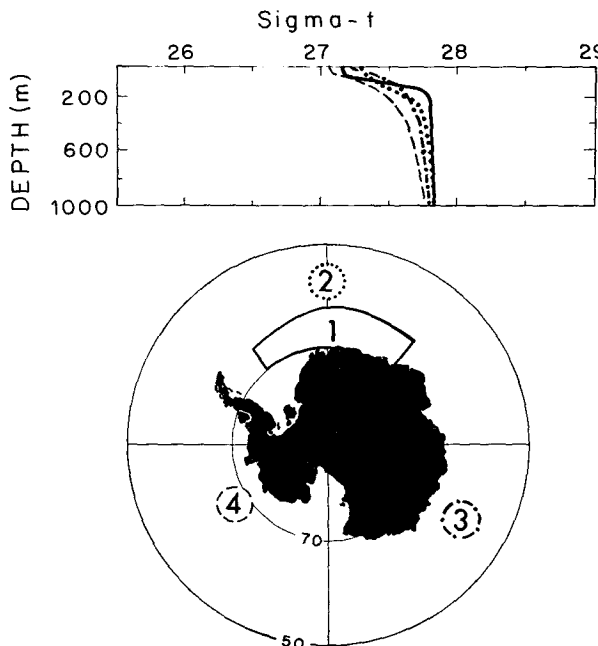


FIG. 2. Averaged sigma- $t$  versus depth profiles for the indicated regions around Antarctica. Notice the distinct two-level character in the region from  $\sim 65^\circ\text{--}70^\circ\text{S}$ , and  $40^\circ\text{E--}40^\circ\text{W}$  (taken from Gordon and Baker, 1981).

arly with depth in the surface level which arguably is a better fit to the data of Fig. 2. This rejection, as well as rejection of a continuous stratification, stems from the following. Whereas non-penetrative mixed-layer models can be applied successfully to a continuously stratified surface cooling situation where deep convection occurs (Killworth, 1976, 1979), there is little known about the modeling of a surface warming situation. How, for example, is the vertical stratification reestablished when there is vertical homogeneity, little surface wind input (such as under near stationary ice) and the surface buoyancy input is stabilizing? In the Medoc situation (Killworth, 1976) this occurs within two weeks of the termination of convection and seems to involve a complicated horizontal interleaving of water masses from outside the convective area. In other words, a sudden return to a thin mixed layer on some Monin-Obukhov scale does not seem to occur. Such effects may also occur in the Weddell polynya although their time scale might well be longer. In the context of a purely vertical model interleaving and recreation of a stable stratification must be parameterized into a single return-to-normal situation and this we have taken as a return to the two-level situation.

This simplification will obviously modify the timing of certain events (at times of overturn, of course, the model will be totally accurate). For example, immediately after convective overturn the initial phase of ice melting will create a surface layer of less dense,

cold, fresh water directly beneath the ice. This would tend to act as an insulator between ice and deeper water. There, however, must be a fairly strong ice motion due to the atmospheric divergence effect. Even a weak stirring by ice keels will maintain a mixed layer of several tens of meters depth (see Lemke, 1979). A calculation along the lines of Section 6 shows that if this is more than  $\sim 25$  m thick, phenomena are produced which are qualitatively similar to those for a single surface level but at a slightly altered time of year. We choose to omit these variations therefore, both for the sake of a simple model and because the effects of such stirring or wave damping by thin sheets of frazil ice are simply not yet well enough understood to include in a model. In any case, the variations are considered to be minor and of little concern here except as noted in that the polynya may tend to refreeze faster than predicted by the model. We maintain though, that conservation of heat and salt within the system ensures that the main physical features of a continuously stratified system are reproduced by the model.

Finally, the two-level approximation has two distinct advantages. First, by using two discrete levels with averaged characteristics, the effects of a steady upwelling will be incorporated into the model through either the thickness or temperature and salinity of the upper level. Second, the dynamics and mechanism of the preconditioning can be ignored as their effects will also be incorporated into the levels.

This two-level approximation confines the model at any time to one of four possible states (Fig. 3). These basic states are as follows. There may be no ice present (states 1 and 2) or ice cover may exist (states 3 and 4). When ice cover exists it is assumed complete. The system may also be statically stable (states 2 and 4) in the sense that the surface density is less than the underlying density, or actively overturning (states 1 and 3) when the system has a vertically uniform density.

In the ice-free states the surface level gains or loses buoyancy through a forcing heat flux  $Q_w(t)$ , where  $t$  represents time, and a constant freshwater input  $f$  due to excess precipitation over evaporation, continental runoff and ice import/export. When ice is present, the system gains or loses a much reduced amount of heat  $Q_i(t)$ , due to the insulating and albedo effects. Further the freshwater input  $f$  accumulates on the ice as snow and is released when the ice is finally melted. For convenience  $f$  has been redefined by the approximate formula  $F = f \times 35\%$ , where  $f$  has normal units for precipitation, of velocity. In this form  $F$  is now defined in terms of a salinity flux and can therefore be directly incorporated into the salinity equations.

In the statically stable states there are transfers of heat and salt between the two levels of the form  $K_T(T_2 - T_1)$  and  $K_S(S_2 - S_1)$ , respectively. Here  $K_T$  and  $K_S$  (which have units of velocity) represent exchange coefficients which include the possible effects of upwelling, turbulent exchange and double diffusion (a level model permits mass transfer between layers). The surface level has temperature  $T_1$  and salinity  $S_1$  and the lower level has quasi-permanent temperature  $T_2$  and salinity  $S_2$ . The latter only change during times of overturn (taking values of  $T$  and  $S$ ) but "snap" back to their usual values when convection ceases. In this way we crudely model the export of the new water mass from the area.

In the ice-covered states, transfers of heat and salt also occur due to exchanges between the upper level and the ice. Following Welander (1977) and Killworth (1979), the heat flux is accomplished through a turbulent exchange coefficient  $K$  and is of the form  $K(T_1 - T_f)$ , where  $T_f$  represents the freezing point of seawater. The salt flux occurs because of the rejection of salt during the ice formation process. This is of the form  $\sigma A$ , where  $A$  is the rate of ice formation due to heating, cooling and excess precipitation as snow and  $\sigma$  is a constant (for simplicity) representing the salinity difference

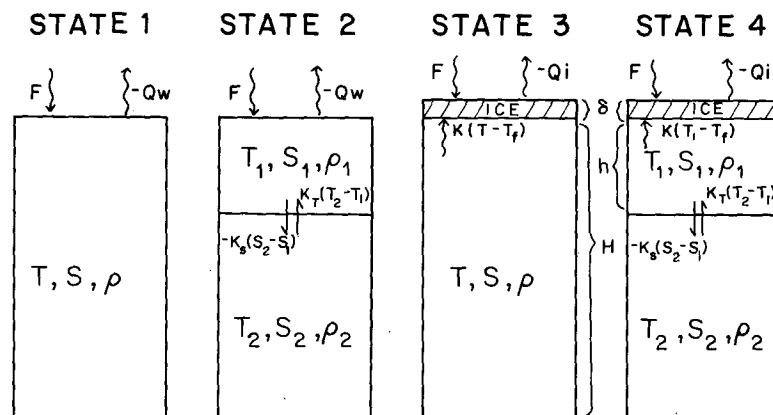


FIG. 3. Schematic representation of the four model states. Sign conventions are noted and symbols are as described in the text.

between the seawater and ice. Denoting the ice thickness by  $\delta$ ,  $A$  becomes  $d\delta/dt = F/\sigma$ ,<sup>2</sup> where the last term represents precipitation.

The equations governing the system are as follows:

STATE 1:

$$H \frac{dT}{dt} = \frac{Q_w}{\rho_0 C_p} \quad (3.1a)$$

$$H \frac{dS}{dt} = -F \quad (3.1b)$$

$$\delta = 0. \quad (3.1c)$$

STATE 2:

$$h \frac{dT_1}{dt} = \frac{Q_w}{\rho_0 C_p} + K_r(T_2 - T_1) \quad (3.2a)$$

$$h \frac{dS_1}{dt} = K_s(S_2 - S_1) - F \quad (3.2b)$$

$$\delta = 0. \quad (3.2c)$$

STATE 3:

$$H \frac{dT}{dt} = -K(T - T_f) \quad (3.3a)$$

$$H \frac{dS}{dt} = \sigma \frac{d\delta}{dt} - F \quad (3.3b)$$

$$\frac{d\delta}{dt} = \frac{1}{\rho_i L} [-Q_i - \rho_0 C_p K(T - T_f)] + F/\sigma. \quad (3.3c)$$

STATE 4:

$$h \frac{dT_1}{dt} = K_r(T_2 - T_1) - K(T_1 - T_f) \quad (3.4a)$$

$$h \frac{dS_1}{dt} = \sigma \frac{d\delta}{dt} - F + K_s(S_2 - S_1) \quad (3.4b)$$

$$\frac{d\delta}{dt} = \frac{1}{\rho_i L} [-Q_i - \rho_0 C_p K(T_1 - T_f)] + F/\sigma. \quad (3.4c)$$

In the above equations  $\rho_0$  represents the mean density of seawater,  $C_p$  its specific heat,  $\rho_i$  the mean density of ice with latent heat  $L$  and  $h$  is the depth of the upper level. Also, it is noted that all of the heat is used to melt or create ice, none is stored within the ice.

Finally, we define an effective equation of state for density  $\rho$  as

$$(\rho - \rho_0)/\rho_0 = -\alpha T + \beta S,$$

where  $\alpha$  and  $\beta$  are constants. The true equation of state is more complicated involving pressure-dependent terms and nonlinearity. Over most of the

<sup>2</sup> This form ensures that the net salinity change in the upper level following ice melt is precisely what it would have been had the precipitation fallen as fresh water.

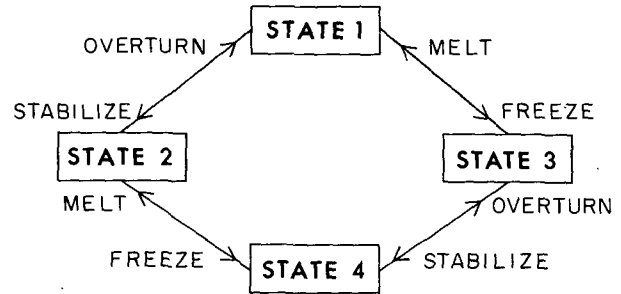


FIG. 4. Summary of the transitions between the model states.

Antarctic region however, the effect of these terms appears to be that overturning occurs when mixing has reached  $\sim 200$  m (Killworth, 1979). Because of this and the fact that we are only comparing densities at the depth  $h$ , the differences between potential and *in situ* values are irrelevant as are the depth dependent terms.

Solutions to (3.1)–(3.4) are straightforward but analytically tedious and not enlightening. They therefore are omitted here for brevity.

#### 4. Transitions between states

Although the governing equations are linear, nonlinearities arise from the abrupt transitions between states which can occur if various conditions are satisfied. These transitions, the conditions which induce them and the initial conditions of the newly entered state (denoted by a prime) are outlined below and summarized in Fig. 4.

The ice free and actively overturning state 1 may stabilize and enter state 2 if the net rate of density change becomes negative. Thus,

$$\text{state 1} \rightarrow \text{state 2} \quad \text{if} \quad -\alpha dT/dt + \beta dS/dt < 0$$

$$T_1' = T; \quad S_1' = S; \quad \delta' = 0.$$

Alternatively, if  $T$  reaches freezing, ice forms and state 3 is entered:

$$\text{state 1} \rightarrow \text{state 3} \quad \text{if} \quad T = T_f$$

$$T' = T_f; \quad S' = S; \quad \delta' = 0.$$

State 2 will overturn and enter state 1 if the upper level density reaches that of the lower level. Thus,

$$\text{state 2} \rightarrow \text{state 1} \quad \text{if} \quad -\alpha(T_1 - T_2) + \beta(S_1 - S_2) = 0$$

$$T' = \bar{T}; \quad S' = \bar{S}; \quad \delta' = 0.$$

{The bar denotes the vertical average of a variable  $\phi$ :  $\bar{\phi} = [h\phi_1 + (H - h)\phi_2]/H$ .}

If  $T_1$  reaches freezing, ice forms and state 4, the ice-covered equivalent to state 2, is entered:

$$\text{state 2} \rightarrow \text{state 4} \quad \text{if} \quad T_1 = T_f$$

$$T_1' = T_1; \quad S_1' = S_1; \quad \delta' = 0.$$

TABLE 1. Average sea-air heat flux for open water ( $Q_w$ ) and ice covered ( $Q_i$ ) conditions for the 60–70°S belt (from Gordon, 1981).

Month	$Q_w$ (W m <sup>-2</sup> )	$Q_i$ (W m <sup>-2</sup> )
Jan	+81	+81
Feb	+11	+11
Mar	-39	-8
Apr	-138	-32
May	-148	-25
Jun	-178	-21
Jul	-206	-25
Aug	-171	-16
Sep	-118	-8
Oct	-49	-7
Nov	+13	+13
Dec	+47	+47

The ice-covered state 3 will enter state 1 if the ice melts:

$$\text{state 3} \rightarrow \text{state 1} \quad \text{if} \quad \delta = 0$$

$$T' = T; \quad S' = S; \quad \delta' = 0,$$

or, if the system stabilizes state 4 is entered:

$$\text{state 3} \rightarrow \text{state 4} \quad \text{if} \quad -\alpha dT/dt + \beta dS/dt < 0$$

$$T_1' = T; \quad S_1' = S; \quad \delta' = \delta.$$

Finally, state 4 may lose its ice and go to state 2:

$$\text{state 4} \rightarrow \text{state 2} \quad \text{if} \quad \delta = 0$$

$$T_1' = T_1; \quad S_1' = S_1; \quad \delta' = 0,$$

or overturn and enter state 3:

$$\text{state 4} \rightarrow \text{state 3} \quad \text{if} \quad -\alpha(T_1 - T_2) + \beta(S_1 - S_2) = 0$$

$$T' = \bar{T}; \quad S' = \bar{S}; \quad \delta' = \delta.$$

It should be noted that some states may be entered only momentarily. For example, ice formation in state 4 may lead to overturning and the transition to state 3. If melting then ensues, the surface density may be stabilized so that state 4 is immediately reentered, but with a new temperature and salinity,  $\bar{T}$  and  $\bar{S}$ . Of course, this overturn would not have been instantaneous. With vertical velocities like those observed in the Mediterranean by Voorhis and Webb (1970) of  $\sim 0.1 \text{ m s}^{-1}$ , it would require approximately half a day to move water particles from top to bottom. For seasonal time scales, however, such a transition is essentially instantaneous.

It also should be observed that the transition from state 1 to state 3 should never occur as the entire water column would be required to cool to the freezing point before the transition would actually take place.

## 5. Parameter values and forcing functions

The depth of the upper level has been chosen to be 200 m for two reasons. First, 200 m is a good ap-

proximation to the summertime observations (Fig. 2). Second, as noted, in a continuously stratified model of surface cooling near the polynya region, Killworth (1979) found that overturning occurred almost invariably after non-penetrative mixing had reached 195–200 m. This upper level depth is clearly a parameter of the model and the effects of varying it will be evaluated later. The total depth  $H$ , is constant at  $4 \times 10^3 \text{ m}$ .

The surface heat exchange values are, needless to say, difficult to obtain in the Antarctic except for localized observations. The values of  $Q_w$  (open ocean) and  $Q_i$  (full ice cover) used in this model (Table 1) are the monthly values given by Gordon (1981) with modifications to the summer insulated values. The  $Q_i$  values for the summer months have been set equal to the  $Q_w$  values. This reflects the large amount of open ocean which is characteristic of the summer ice and which forces the summer  $Q_i$  values to nearly equal those for open ocean (Fletcher, 1969). The actual values are undoubtedly some compromise between these two extremes. Without modification however, the ice generated in the winter would never melt (in the absence of overturning).

The freshwater input  $f$  is an even more difficult value to attain. The major source of  $f$  is precipitation over evaporation ( $P - E$ ). Continental runoff  $R$  and ice import from the surrounding ice field  $I$  comprise secondary sources. Several references are available which give estimated values of  $P - E$ . Wust *et al.* (1954) estimate a value of  $0.4 \text{ m year}^{-1}$  for the region south of the polar front. van Loon, in his 1972 review, presents Albrecht's  $P - E$  map which extends only to 60°S. At this latitude the value is slightly less than  $0.5 \text{ m year}^{-1}$ . Newton (1972) indicates a  $P - E$  for 60–70°S of  $0.27 \text{ m year}^{-1}$ . Loewe (1967) states that the Antarctic seas have a high precipitation of order  $1 \text{ m year}^{-1}$  which diminishes towards the coast. His value, combined with Gordon's (1981) evaporation values of  $0.2\text{--}0.4 \text{ m year}^{-1}$  yields a  $P - E$  range of  $0.6\text{--}0.8 \text{ m year}^{-1}$ . We therefore obtain a total range for a  $P - E$  input of  $0.27\text{--}0.8 \text{ m year}^{-1}$ .

Continental runoff values are given by van Loon (1972) who presents estimates of a net precipitation of  $0.11\text{--}0.19 \text{ m year}^{-1}$  over Antarctica. Most of this melts south of 60°S (i.e., not many icebergs are reported north of 60°S) where the ocean area is about equal to the Antarctic area ( $\sim 14 \times 10^6 \text{ km}^2$ ). A freshwater input by melting glacial ice  $R$  may therefore be taken as  $0.11\text{--}0.19 \text{ m year}^{-1}$ .

The effects of sea-ice import from the surrounding ice field can only be roughly estimated at best. Evidence for this estimate is derived through examination of the weekly satellite photos (from which Fig. 1 was based) which show no significant increase in the polynya's areal extent during its existence each year prior to spring breakup in November. An increase might be expected if a significant portion of the ice along the polynya's perimeter were continuously

drifting into the polynya area and melting. This of course ignores the fact that the newly cleared perimeter could be refreezing or receiving in-drifting ice itself during this period. If the later of these was occurring though, the areal extent of the transition zone separating the ice-free polynya from the more densely packed surrounding ice field should itself show an increase over the winter. Examination of the microwave satellite images for the major polynya years of 1974–76 show that this transition zone maintains a near constant areal extent from the time the polynya first forms until the spring breakup. Therefore, if any appreciable area of ice were to drift into the polynya without showing up on the satellite records, a refreezing would be required in the transition zone. If this were the case the in-drifting, newly formed ice would be only centimeters thick and thus its volume considerably reduced.

Based on this discussion it would appear that ice import into the polynya region is not substantial. This is consistent, with the polynya induced divergent wind field, discussed previously, which would be expected to help maintain nearly ice-free conditions. A lower limit for this component of the freshwater input can therefore be taken as  $0 \text{ m year}^{-1}$ .

As an upper limit we estimate that at most an area of ice equal to that of the polynya could drift into the polynya without being detected by examination of the satellite data. Much of this ice, in fact, could be derived from the transition zone which averages  $\sim 50\%$  ice concentration and whose areal extent is approximately twice that of the polynya. Therefore, conceivably some of this "missing" ice from the transition zone could have drifted into and melted within the polynya (not all of this could have drifted in because the transition zone is present in roughly its full extent as soon as the polynya is formed). For ice  $\sim 1 \text{ m}$  thick and with a salinity of  $5\%$  this would contribute  $\sim 0.86 \text{ m}$  of fresh water to the polynya. This value is high and should easily subsume the effects of in-drifting newly frozen (thin) ice; in-blowing snow from surrounding regions; storm-blown ice input, etc. Averaging over the seven years for which we have data this upper limit becomes  $\sim 0.74 \text{ m year}^{-1}$  (1978 is the only year without a polynya). We thus estimate an ice-import freshwater input<sup>3</sup> ( $L$ ) range of  $0\text{--}0.76 \text{ m year}^{-1}$ ; presumably the lower end of this range is more reasonable.

Combining these values to obtain an overall range ( $P - E + R + I$ ) for the freshwater input results in  $0.38\text{--}1.73 \text{ m year}^{-1}$  for the value of  $f$ . Because of the size of this range we are compelled to treat  $f$  as a

model parameter to be tuned. In converting  $f$  to a freshwater flux  $F$ , as it is used in these calculations, over the basic time unit used here (one day) it is noted that a value of  $0.5 \text{ m year}^{-1}$  is equivalent to approximately  $4.8\%$   $\text{cm day}^{-1}$  (these units are used to maintain values of order 1).

The value of  $K$  (turbulent heat flux coefficient from the water into the ice) is taken from Killworth (1979) in which he derives a value of  $3 \times 10^{-4} \text{ m s}^{-1}$ . This is a large value, in the sense that water maintained at  $1^\circ\text{C}$  above freezing could essentially melt nearly  $0.50 \text{ m}$  of ice per day. We therefore investigate the effect of decreasing  $K$  later.

The values of  $K_T$  and  $K_S$  are less easy to ascribe. The values used here are  $K_T = 7 \times 10^{-7} \text{ m s}^{-1}$  and  $K_S = 10^{-7} \text{ m s}^{-1}$ , where their relative magnitude has been determined assuming double diffusive processes to be important. Indeed, the observed structure of cold fresh water overlying warmer saltier water is ideal for this process. Further, step structures have been observed in the vicinity (Foster and Carmack, 1976). This being the case, one might expect  $K_S \approx 0.15 K_T$  (Turner, 1973), as we have taken here (the model has been run with  $K_S = K_T$  with insignificant changes in the results).

The actual value of  $K_T$  used here was taken from the seasonally averaged Ekman drift-induced vertical velocities at the base of the Ekman layer from Gordon *et al.* (1977). Their Fig. 19 shows that this value varies from  $\sim 1 \times 10^{-6} \text{ m s}^{-1}$  in the winter and spring to  $\sim 5 \times 10^{-7} \text{ m s}^{-1}$  in the summer and fall. Our value is then the approximate average of these values, i.e.,  $7 \times 10^{-7} \text{ m s}^{-1}$ .

Alternatively estimates of these transfer coefficients can be calculated by using the above as well as different interpretations as to their physical origin. This has been done as a check on their magnitude attained above. If one assumes  $K_T$  and  $K_S$  are products of a mean upwelling velocity  $w$ , then a two-level truncation of the Bryan (1969) finite-difference scheme, neglecting horizontal  $T$  and  $S$  derivatives, yields

$$h\phi_t = \frac{1}{2}w(\phi_2 - \phi) \quad (5.1)$$

for a variable  $\phi$ . With  $w/2 = K_T$ , we can check the magnitude of our estimate by solving for a variable  $\phi$ . Setting  $w/2 = K_T$  yields a value of upwelling of  $\sim 1.4 \times 10^{-6} \text{ m s}^{-1}$ ; with  $w/2 = K_S$ , the value is  $\sim 2.1 \times 10^{-7} \text{ m s}^{-1}$ . These solutions average to  $\sim 8 \times 10^{-7} \text{ m s}^{-1}$  and are thus in good agreement to the values of Gordon *et al.* (1977), although polynya-induced Ekman divergence could yield higher values, as could topographic effects.

If  $K_T$  and  $K_S$  are instead assumed to be solely the effects of vertical turbulent exchanges with some vertical transfer coefficient  $K_v$ , the finite differencing would yield

$$h\phi_t = 2K_v H^{-1}(\phi_2 - \phi). \quad (5.2)$$

<sup>3</sup> This input is obviously asymmetrical with respect to time, occurring only during the winter months of the year and only in years in which a polynya occurs. The timing of the freshwater input over the course of a year is irrelevant though as only the net input over the year is of importance. The yearly variation is more important and is examined in Sections 7 and 8.



Setting  $2K_v/H = K_T$  yields  $K_v \sim 1.4 \times 10^{-3} \text{ m}^2 \text{ s}^{-1}$ ; with  $2K_v/H = K_S$  the value is  $2 \times 10^{-4} \text{ m}^2 \text{ s}^{-1}$ . Here the latter value is more widely accepted in the literature and for our value of  $h$  also is in good agreement to the above estimates. If  $K_T$  and  $K_S$  represent simple return-to-normal relaxation parameters (e.g., long-term horizontal advection), the values used correspond to relaxation times  $h/K_T$ ,  $h/K_S$  of 9 and 61 years, respectively.

It is because all these physical effects exist that we choose to include the  $K_T$ ,  $K_S$  terms in the model, but it is obvious that totally acceptable estimates of their values are difficult. Fortunately, insight as to the sensitivity of the model with respect to the values of  $K_T$  and  $K_S$  can be obtained through a simple scale analysis. For example, in Eq. (3.2b), the importance of salt diffusion with respect to freshwater input in state 2 is measured by the ratio  $K_S \Delta S / F$ , where  $\Delta S$  is the magnitude of  $(S_2 - S_1)$ . The value of  $\Delta S$  is  $\sim 0.2\text{‰}$  and  $F$  can vary from as low as  $\sim 4\text{‰ cm day}^{-1}$  to as high as  $\sim 17\text{‰ cm day}^{-1}$ . As a result, the salt diffusion is less than 5% of the freshwater input effect and therefore can be ignored without a significant loss of accuracy.

The importance of salt diffusion with respect to salt rejection, in state 4, is measured by  $K_S \Delta S \rho_i L / \sigma \bar{Q}_i$  as determined by Eqs. (3.4b) and (3.4c). Here the bar signifies the average value. For this case the ratio is  $\leq 0.01$  and therefore  $K_S$  can essentially be neglected in this state as well.

As with  $K_S$ ,  $K_T$  has relevance only in states 2 and 4. In state 2, the governing ratio  $\rho_0 C_p K_T \Delta T / \bar{Q}_w$  is  $\sim 0.03$ , where  $\Delta T$  is the magnitude of  $(T_2 - T_1)$ . From this, the heat diffusion is seen to be of minor importance and can thus be neglected.

In state 4 the situation is more subtle and depends on whether ice is forming or melting. If it's melting following an overturn (therefore, inducing a return to state 4),  $T_1$  is near  $T_2$  and  $K(T_1 - T_f) \gg K_T(T_2 - T_1)$  in (3.4a). The  $K_T$  term is therefore negligible. During freezing, however,  $T_1$  is near  $T_f$ . In fact, after a time scale of  $O(h/K)$ , about 10 days,  $T_1$  becomes asymptotic to a value such that

$$K(T_1 - T_f) \approx K_T(T_2 - T_f); \quad T_1 \approx T_f.$$

This effect is felt in (3.4c) as a heat input to the ice which retards its growth. The importance of this term is then measured by the ratio

$$\frac{\rho_0 C_p K(T_1 - T_f)}{\bar{Q}_i} \approx \frac{\rho_0 C_p K_T(T_2 - T_f)}{\bar{Q}_i} \quad (5.3)$$

$$\approx 0.17 \text{ (midwinter) to } 0.78 \text{ (late spring).}$$

This non-negligible amount therefore prevents the neglect of  $K_T$  from the model without a loss in accuracy.

It will be useful, however, for several purposes to consider a "pure" model in which we do set  $K_T$  and

$K_S$  to zero,  $K$  to infinity (i.e., immediate melting following an overturn) and  $H$  to infinity. This pure model is then parameter free and its use in Section 6 will permit analysis of the system and isolation of the important parts of its physics.

The initial conditions and fixed model parameters can now be discussed. Initial values for  $T_1$  and  $S_1$  have been derived from observations. In order to facilitate the comparison between the model results and the actual observations, values have been chosen which are thought to be most representative of those in the polynya area during the initiation of ice formation in 1973. The value of  $T_1'$  was thus obtained through an examination of satellite photos which indicate that sea-ice began to form in the polynya area on or near 15 June 1973. Our model therefore begins on 15 June with  $T_1' = T_f$ .

The initial salinity value is more difficult to ascribe and we choose to treat it as an adjustable initial condition. The lower limit is set by the 20 m depth, local summer salinity of 34.4‰ (Gordon and Molinelli, 1981). As the summer value should represent the lowest value seasonally and the 20 m depth value, the lowest value vertically (neglecting the surface which is subject to extreme local fluctuations), this value should represent a safe lower limit. The effects of the various values of  $S_1'$  possible will be discussed in Section 6.

Finally, the fixed parameters are:  $T_2 = 0^\circ\text{C}$ ;  $S_2 = 34.66\text{‰}$ ;  $\rho_i = 900 \text{ kg m}^{-3}$ ;  $L = 2.5 \times 10^5 \text{ J kg}^{-1}$  (for sea ice salinity of 5‰);  $\rho_0 = 10^3 \text{ kg m}^{-3}$ ;  $C_p = 4.18 \times 10^3 \text{ J kg}^{-1} \text{ }^\circ\text{C}^{-1}$ ;  $\sigma = 30\text{‰}$ ;  $T_f = -1.86^\circ\text{C}$ ;  $\alpha = 5.82 \times 10^{-5} \text{ }^\circ\text{C}^{-1}$  and  $\beta = 8 \times 10^{-4} \text{‰}^{-1}$ .

Owing to the paucity of data in the region of the polynya (especially during winter) the parameter values derived and estimated in this section are obviously provisional. We feel, however, that the values are adequate for an initial testing of the simple model. If successful the model can then be tested as to its sensitivity to these various parameters. If the model can tolerate a reasonable range of parameter values it can then be assumed feasible. Further development, including higher order physics, is then warranted at which point the model will justifiably require more precise parameter estimates. At this stage of development though, the values attained should satisfactorily serve as starting points. Examination of possible ranges in the values and their effects on the model results are presented in Section 8.

## 6. Sensitivity to parameters and a model analysis

### a. Time-evolving $T - S$ representation

The properties of (3.1)–(3.4) are most easily understood when represented on a time-evolving  $T - S$  diagram. Such a diagram is presented in Fig. 5 which depicts the various seasonally averaged trends pos-

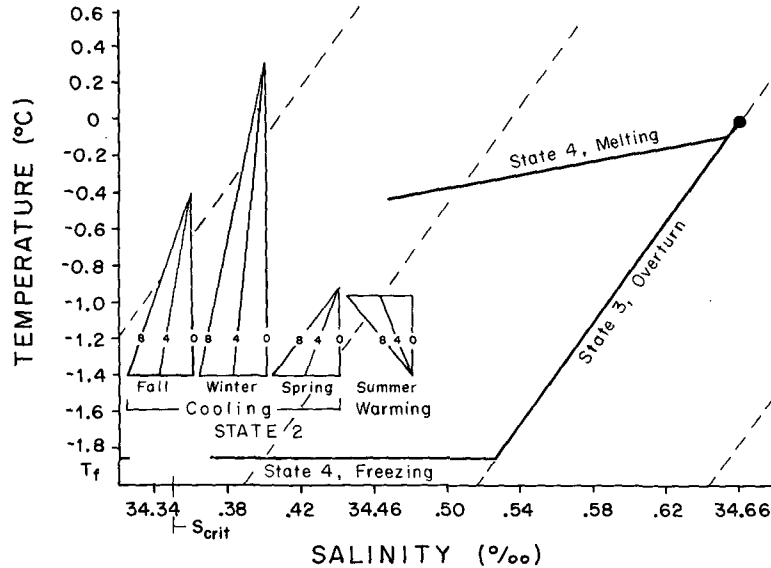


FIG. 5. Time evolving  $T-S$  diagram depicting the various trends possible in the four states of the model. The slopes followed during times of open water (state 2) appear as seasonally averaged "triangles" with the actual slope dependent on the value of  $F$  (shown here for  $F = 0, 4$  and  $8‰ \text{ cm day}^{-1}$ ). State 1 occurs when one of the cooling state 2 slopes directly intersects the overturn slope. If they instead intersect the freezing slope first, overturn occurs in state 3. Melting occurs in state 4 and is directly followed by a state 2 slope. The actual distance traversed on any one slope depends on the length of time spent in the specific state. Isopycnals are represented by the dashed lines.

sible in the model over the range of  $F$  previously described. In state 2, the slopes and time scales can be deduced by simplifying (3.2a, b, c). Neglecting  $K_T$  and  $K_S$ , division of (3.2a) by (3.2b) yields the slope traversed by the upper level water mass on a  $T-S$  diagram:

$$\text{state 2: } \frac{dT_1}{dS_1} = -Q_w / \rho_0 C_p F. \quad (6.1)$$

Comparison of these slopes with the isopycnals (which are parallel and straight due to the simplified equation of state and narrow  $T-S$  range) in Fig. 5 show that summer and spring, if  $F \geq 8‰ \text{ cm day}^{-1}$ , are the only seasons in which the upper level buoyancy is increased and the system becomes more stable. During the other two seasons, unless there is an extremely high rate of freshwater input, the cooling dominates the buoyancy flux and the upper level increases in density. The speed, on the other hand, at which the curve (6.1) is traversed depends on the cooling rate, (3.2b). The changes  $\Delta T_1$  and  $\Delta S_1$  over a time interval  $t$  are thus:

$$\begin{aligned} \text{state 2: } \Delta T_1 &= (h \rho_0 C_p)^{-1} \int Q_w dt, \\ \Delta S_1 &= -Ft/h, \end{aligned} \quad (6.2)$$

where the integral is evaluated over the time interval concerned.

State 4 trends and time scales are similarly obtained using (3.4a, b, c). When state 4 is entered  $T_1 = T_f$  and (3.4a) shows that  $dT_1/dS_1$  vanishes if  $K_T$  is zero [if  $K_T$  is nonzero (5.3) shows that  $dT_1/dS_1$  remains very small]. Movement along the line  $T_1 \approx T_f$  is thus governed by changes in  $S_1$  due to ice growth. By (3.4b, c):

state 4 (freezing):

$$\frac{\sigma}{h} \delta = \Delta S_1 = \frac{-\sigma}{h \rho_i L} \int Q_i dt, \quad (6.3)$$

if  $K_T$  is zero. If  $K_T$  is nonzero, then:

state 4 (freezing):

$$\frac{\sigma}{h} \delta = \Delta S_1 \approx - \frac{\sigma}{h \rho_i L} \int Q_i' dt. \quad (6.4)$$

Here  $Q_i'$  is a modified cooling rate due to heat transfer from the water which is given to a good degree of approximation by (5.3):

$$Q_i' = Q_i + \rho_0 C_p K_T (T_2 - T_f) = Q_i + 5.36 \text{ W m}^{-2}. \quad (6.5)$$

From (6.4),  $S_1$  and  $\delta$  increase during cooling and overturn will occur when  $S_1$  reaches a value  $S_{ov}$ . This is given by the requirement that  $\rho_1 = \rho_2$ , with a freezing upper level.  $S_{ov}$  is then determined from the equation of state as

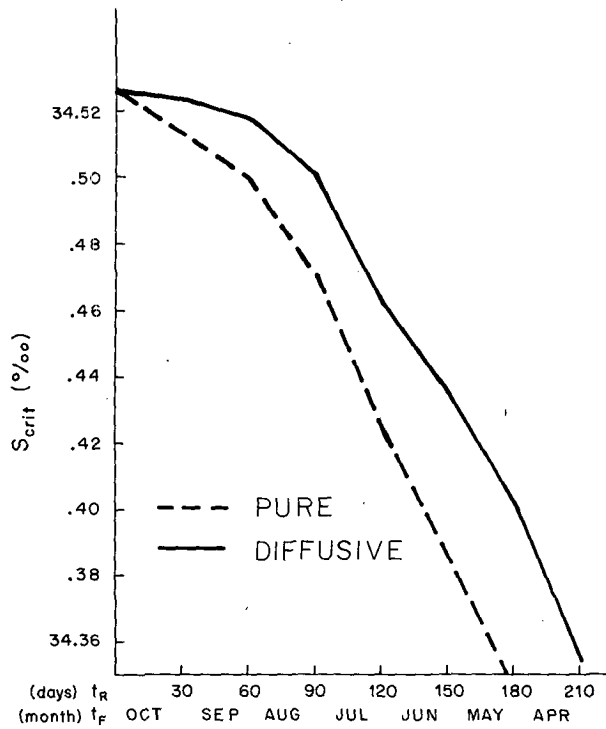


FIG. 6. Plot of  $S_{crit}$  as a function of the time remaining in the cooling season after ice onset ( $t_R$ ) or the month in which freezing begins ( $t_F$ ).

$$S_{ov} = S_2 + \alpha\beta^{-1}(T_f - T_2) = 34.526\text{‰}. \quad (6.6)$$

During overturning (state 3)  $T_1$  and  $S_1$  take their depth-averaged values of  $-0.09^\circ\text{C}$  and  $34.652\text{‰}$ , respectively. Melting in state 4 then ensues. Since  $K(T_1 - T_f) \gg \rho_0 C_p Q_i$ , (3.4c) shows that the system moves along the line:

$$\text{state 4 (melting): } \frac{dT_1}{dS_1} = \frac{\rho_i L}{\sigma \rho_0 C_p} = 1.8^\circ\text{C‰}^{-1} \quad (6.7)$$

in a time  $t$ . This is then given to a good degree of approximation by the amount of ice present

$$t = (\rho_i L \delta) / [\rho_0 C_p K (T_2 - T_f)], \quad (6.8)$$

about  $1.1 \text{ days m}^{-1}$  of ice.

Based on this discussion we can determine whether or not the system overturns (assuming proper pre-conditioning) in any one particular year. For any time of ice onset (say,  $t_r$  days before the onset of summer heating on day  $t_s$ ), there is a critical salinity  $S_{crit}$  given by

$$S_{crit} = S_{ov}$$

$$+ \frac{\sigma}{\rho_i L h} \int_{t_s - t_r}^{t_s} Q_i dt \quad (\text{non-diffusive or pure})$$

or

$$S_{crit} = S_{ov} + \frac{\sigma}{\rho_i L h} \int_{t_s - t_r}^{t_s} Q_i' dt \quad (\text{diffusive}), \quad (6.9)$$

such that if  $S_1 \geq S_{crit}$  at ice onset the system will overturn before the end of the cooling and if  $S_1 < S_{crit}$  there will be no overturn that season. The value of  $S_{crit}$  as a function of  $t_R$  as well as time of ice onset ( $t_F$ ) is plotted in Fig. 6. For the first year of the model, since ice begins to form on 15 June, we would expect an  $S'_{crit} \sim 34.45\text{‰}$ . Conceivably, state 4 could be entered at the beginning of March (if overturn had not occurred during winter and the summer heating was used to remove the ice) yielding an overall minimum  $S_{crit}$  of  $34.35\text{‰}$ . In other words, if  $S_1$  ever becomes less than this value, overturn will not occur again.

These considerations show that the behavior of the system is sensitive to the times spent in the various cycles and to the times in the seasons when the various cycles are entered. A year without overturn makes the upper level colder (but fresher) than if the warm deep water had been mixed into the upper level and thus induces an early ice onset the following year. From Fig. 6, this tends to increase the probability of an overturn in the ensuing winter due to the longer time available for ice formation. Similarly, a year with a polynya may well be followed by a year without one due to the net warming or, several years with polynyas may each successively raise the surface temperature enough to prevent one from forming the next year, etc.

How frequently one might expect an overturn to occur depends mainly on  $F$ . Over the period of one year (assuming open water to have occurred allowing winter  $F$  to be transferred) the salinity content of the upper level decreases by  $F \times (\text{one year})$ . There is also an increase due to salt diffusion but this is negligible. When an overturn occurs, the total salinity content  $hS_1$  of the upper level is increased by an amount

$$\frac{H - h}{H} h(S_2 - S_{ov}) = 25.62\text{‰ m}.$$

Of course, the frequency of overturning may be entirely erratic. In a single cooling season an overturn may occur in early fall, late winter, twice or not at all. Regardless, however, if there are  $p$  overturns in  $n$  years, then a rough salinity balance is achieved when

$$nF \times (1 \text{ year}) = 25.62p \quad \text{or} \quad F \approx 7p/n,$$

that is, a yearly freshwater input rate of  $\sim 0.73(p/n)m$ . This formulation therefore enables us to put approximate bounds on the overturning frequency. The maximum freshwater input of  $1.73 \text{ m year}^{-1}$  requires 16 overturns in seven years to achieve a

salinity balance; the minimum value of  $0.38 \text{ m year}^{-1}$  four overturns in seven years.<sup>4</sup> The seven years from 1973 to 1979 had six overturns (ignoring the 1979 eastern polynya for reasons to become obvious later) from which we might expect that if a salinity balance was achieved the net freshwater input was  $\sim 0.63 \text{ m year}^{-1}$ ; if the 1979 western ice degradation was an overturn then this value would be  $\sim 0.73 \text{ m year}^{-1}$ .

Finally, if the freshwater input exactly balances the salinity increase due to overturning so that overturn occurs regularly (e.g., once a year), an ideal seasonal cycle can be constructed. An analysis of such a seasonal cycle is in itself extremely beneficial. More complicated cycles also can be analyzed such as four polynyas every seven years but with little additional insight.

### b. Analysis of the seasonal cycle

We consider the simple cycle shown in Fig. 7 and the pure model discussed in Section 5. For clarity the subscript 1 has been removed from  $T_1$  and  $S_1$  as state 3 is only entered momentarily and the subscripts  $F$  (freezing),  $OT$  (overturn),  $PM$  (pre-ice melt),  $P$  (polynya) and  $W$  (warming) correspond to the respectively labeled positions in Fig. 7. At time  $t_F$ , freezing begins and state 4 is entered. Freezing and ice growth continues until  $t_{OT}$  at which time  $S_1 = S_{ov}$  and the system overturns. Recall that in the pure model  $H$  (the reservoir depth) and  $K$  (coefficient of heat transfer into the ice from the water) are both infinite, hence on overturning the resulting mixture is  $T_2$  and  $S_2$  and the ice melts instantly to point  $P$ . A polynya is now formed (state 2 is entered) as there is no ice while still in the midst of the cooling season (when ice is still present elsewhere). This polynya condition continues until point  $W$  at which time the warming cycle begins and the surrounding ice fields disappear. The system remains in state 2 through this warming and into the fall cooling period until a time  $t_{F'} \equiv (t_F + 1 \text{ year})$ .

This system is straightforward to analyze and we note that

$$t_{OT} = t_{PM} = t_P, \quad (6.10)$$

(i.e., overturn is immediately followed by the formation of a polynya)

$$T_{PM} = T_2; \quad T_F = T_{OT} = T_P, \quad (6.11)$$

$$S_{PM} = S_2; \quad S_{OT} = S_{ov} = S_2 + \alpha\beta^{-1}(T_f - T_2). \quad (6.12)$$

Conservation of salt yields a set of relationships as follows. Between  $t_P$  and  $t_F$  the salinity is decreased by the freshwater input:

<sup>4</sup> This does not imply that decreasing the yearly net freshwater input decreases the overturn frequency. This only follows if the system conserves salt (i.e., neither gains or loses salt over the specified period of time).

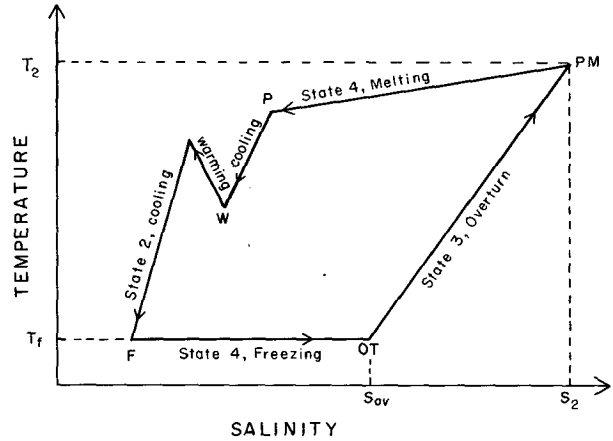


FIG. 7. Schematic representation of a simple one-year cycle on a time evolving  $T-S$  diagram. Labelled positions correspond to freezing ( $F$ ), overturn ( $OT$ ), pre-ice melt ( $PM$ ), polynya initiation ( $P$ ) and end of the polynya upon warming ( $W$ ). The trajectories shown here are straight for convenience.

$$S_F - S_P = [-F(t_F - t_P)]/h. \quad (6.13)$$

Between  $t_F$  and  $t_P$  the salinity is increased by the freezing of sea-ice:

$$\begin{aligned} S_{ov} - S_F &= \frac{\sigma}{h} \delta_{OT} - \frac{F}{h} (t_P' - t_F) \\ &= -\frac{\sigma}{\rho_i L h} \int_{t_F}^{t_P'} Q_i dt. \end{aligned} \quad (6.14)$$

During melting

$$S_P - S_2 = -\frac{\sigma}{h} \delta_{OT}. \quad (6.15)$$

Combining (6.13), (6.14) and (6.15) then yields

$$\begin{aligned} S_{ov} - S_2 &= \frac{\alpha}{\beta} (T_f - T_2) \\ &= \frac{-F(t_P' - t_P)}{h} = \frac{-F(1 \text{ year})}{h} \end{aligned} \quad (6.16)$$

Therefore, this shows that the total gain in freshwater over a single cycle which exactly balances the gain in saline water due to overturning (this  $F$  takes the value  $F_{crit}$ ) is given by

$$F_{crit} (1 \text{ year}) = \frac{\alpha}{\beta} h(T_2 - T_f). \quad (6.17)$$

This is equivalent to a freshwater accumulation over a one-year cycle of  $\sim 0.78 \text{ m}$ ; thus  $F_{crit} = 7.39\% \text{ cm day}^{-1}$ .

Similarly, conservation of heat from  $t_P$  to  $t_F$  yields

$$T_f - T_P = \frac{1}{\rho_0 C_p h} \int_{t_P}^{t_F} Q_w dt. \quad (6.18)$$

A final relation, thus closing the system, is obtained from (3.4a, b, c). Elimination of  $K$  and integrating gives, for the melting from  $PM$  to  $P$

$$S_P - S_2 = \frac{\rho_0 C_p \sigma}{\rho_i L} (T_P - T_2). \quad (6.19)$$

Eliminating all of the unknowns except the times  $t_P$  and  $t_F$ , we obtain

$$T_f - T_2 - \frac{\Sigma Q_i}{\rho_0 C_p h} + \frac{\rho_i L F (1 \text{ year})}{\rho_0 C_p \sigma h} = \frac{1}{\rho_0 C_p h} \int_{t_P}^{t_F} \left( Q_w - Q_i + \frac{\rho_i L F}{\sigma} \right) dt, \quad (6.20)$$

where  $\Sigma Q_i$  is the integrated total of  $Q_i$  over an entire year.

If  $t_P$  is now specified, (6.20) yields  $t_F$  and (6.13)–(6.19) yield the other quantities (subject to minor restrictions such as no second freezing period during the cycle). Fig. 8 shows the range of solutions possible. Note that  $S_P$  and  $S_F$  achieve maximal values as functions of  $t_P$ . In other words for certain salinity values at the onset of freezing ( $S_F$ ), the time of this onset can take two different values (both in mid-winter) and yield two exact yearly cycles. The time of melting, though, does differ between the two by almost a season.

These cycles were for the pure model. If we now restore the values of the diffusion coefficients and lower depth, equivalent cycles can still be constructed but solving for the various parameters involves iterative solution procedures. The effects of diffusion can be approximated by replacing  $Q_i$  with

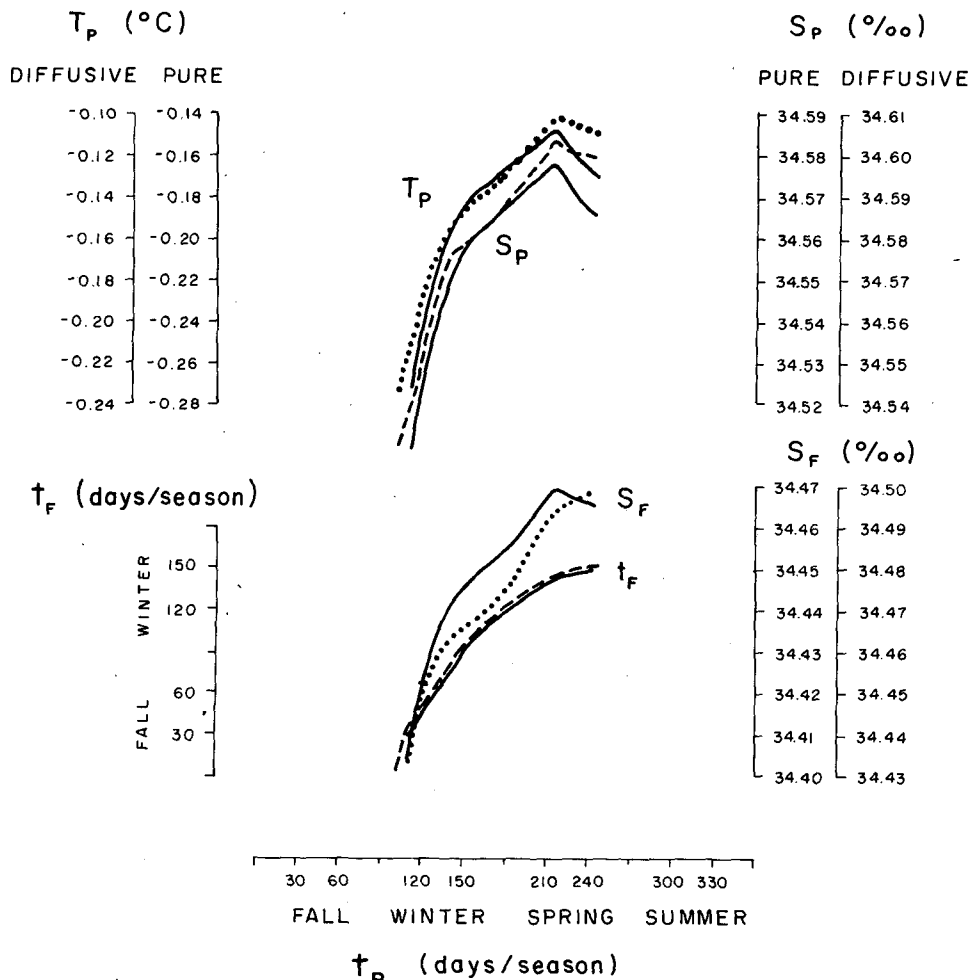


FIG. 8. Range of solutions for the pure model seasonal cycle analysis;  $F = 7.39\% \text{ cm day}^{-1}$ . The actual (diffusive) model solutions have also been approximated (corresponding to  $F \approx 7.59\% \text{ cm day}^{-1}$ ) and are accurate until about  $t_P$  of late spring where they become  $\sim 0.01\%$  too low. They are shown, with their corresponding pure solutions, as dashed or dotted lines. Some smoothing has been applied to the salinities for clarity.

$Q_i'$ , defined in (6.5), which is shown by the dashed lines of Fig. 8. Roughly, this reduces the effective ice formation rate which increases the salinities slightly over their pure values by  $\sim 0.02\text{--}0.03\text{‰}$  as shown by the figure. The value of  $F$  is also increased by  $\sim 0.2\text{‰ cm day}^{-1}$  over its pure value to compensate for the extra salinity input by diffusion.

An examination of the solutions in Fig. 8 reveals several interesting results. First, it is seen that the results here are in agreement with those derived for  $S'_{\text{crit}} \sim 34.45\text{‰}$  in Section 6a (obviously, no solution is obtainable in which a regular seasonal cycle can be obtained with  $S_1' < S'_{\text{crit}}$  as the analysis assumes an overturn occurs each year). It also is interesting to note that there are no one-year cycles in which melting occurs (i.e., the polynya forms) before, say, midwinter, even though the onset of freezing may take place at any reasonable time from about midfall to as late as midwinter. Finally, it is observed that the range in  $S_F (=S_1')$  for the diffusive model is  $\sim 34.43\text{--}34.50\text{‰}$ .

### c. Deviations from the ideal seasonal cycle

From the above discussion it is seen that the ideal annual cycle is very sensitive to the forcing. It is not surprising therefore, to find on further analysis that the system will not remain in this ideal seasonal cycle for two distinct reasons: 1) either the cycle is naturally unstable in that a small perturbation will result in divergence from the original cycle with time, or 2) the forcing for the cycle will change or is not sufficient to achieve or maintain an annual cycle.

The stability of the pure seasonal cycle, discussed in Section 6b is straightforward to analyze. Essentially small perturbations  $\epsilon$  to  $T_1$  and  $\mu$  to  $S_1$  at time  $t_p$  are followed around a year's cycle. After some lengthy algebra it is found that

$$\epsilon' = - \frac{(1 - r_F)(1 + \gamma_P r_P)}{r_P r_F \gamma_F} \epsilon - \frac{\rho_i L}{\rho_0 C_p \sigma} \left( \frac{1 - r_P}{r_P} + \gamma_P \right) \mu. \quad (6.21)$$

where  $\epsilon'$ ,  $\mu'$  are the values of  $\epsilon$  and  $\mu$  one year later and

$$r_{F,P} = \frac{\sigma Q_{iF,P}}{\rho_i L F}, \quad \gamma_{F,P} = \frac{Q_{wF,P}}{Q_{iF,P}} \quad (6.22)$$

are defined by the seasonal solution. Note that  $\mu$  remains unchanged simply because  $F$  takes the value  $F_{\text{crit}}$ . The system is thus stable or unstable according as

$$\left| \frac{(1 - r_F)(1 + \gamma_P r_P)}{(r_P r_F \gamma_F)} \right| \leq 1 \quad (6.23)$$

For the pure model, stability will result from  $t_p$

values in early spring or later (after the maximum in Fig. 8, in fact) and instability results from earlier values. If diffusive effects are introduced, however, all one-year cycles are unstable.

In other words, we can never expect to see steady cycling for many years as irregularities must enter because of the instability. Eventually, an overturn will be missed one year and the system will become less salty. The length of time before this results will depend on the initial amplitude of  $\epsilon$ .

Similar behavior results from an  $F$  which is either greater or less than  $F_{\text{crit}}$ . Fig. 9a shows the situation for  $F > F_{\text{crit}}$ . This increased  $F$  has no effect until the ice melts at which time the increased  $F$  makes  $S_1$  slightly less salty than before. This, plus the extra freshwater input in state 2 results in more winter cooling required to reach overturn. By the following summer the system is both warmer<sup>5</sup> and fresher and therefore requires still more time to reach overturn the following year. As Fig. 9a shows, the salinity at ice onset will be fresher each year, while the time of onset becomes later. It then follows from Fig. 7 that eventually  $S_1$  will be less than  $S_{\text{crit}}$  and no overturn will occur during the year. Hence the system will eventually stabilize itself and become fresher each year (although there may still be a few more overturns following years of no overturn before this onset of stability).

For  $F < F_{\text{crit}}$  (Fig. 9b) the opposite would occur;  $F$  is now decreased thus increasing the salinity of the system and reducing the winter cooling necessary to reach overturn. By the following summer the system is colder and saltier and overturn is reached still sooner the following year. Eventually, the vertical stability is so reduced that state 1 is entered with overturn resulting simply from cooling and no ice forms. Since the overturn removes the freshwater input, a stable cycle of state 2 in the summer and state 1 the remainder of the year is now established.

In both of these cases the number of years required until stable cycling occurs decreases (in a complex fashion) as  $|F - F_{\text{crit}}|$  increases. Similar calculations can be performed with the more complicated multiyear cycles of course, which tend to be more stable than the one-year cycle. However, the above discussion does suggest that unless  $F$  varies as a function of time or is in some way nonconservative, the cycling pattern of the system will be irregular until the system reaches stability.

## 7. Data interpretation and model results

Before results from the complete model can be fully evaluated, it is necessary to have a clear cut

<sup>5</sup> The surface layer loses heat because of an increased melting but gains heat by not being cooled very long in state 2; the ratio of these is  $Q_i/Q_w < 1$ , so the system is warmed.

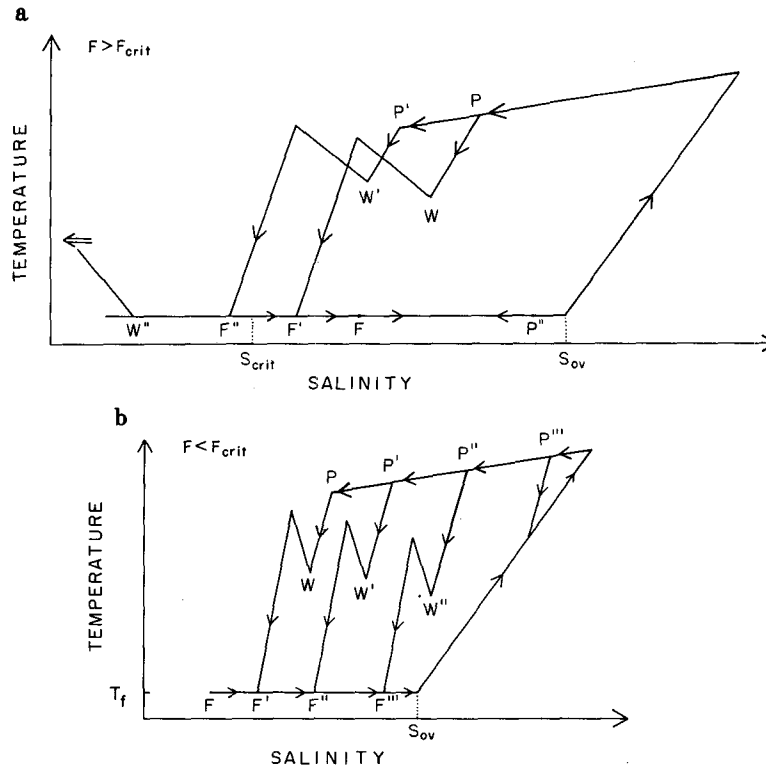


FIG. 9. Schematic representation of (a) stability induced by  $F > F_{crit}$  (eventually enough ice will not be generated to induce overturning) and (b) stability induced by  $F < F_{crit}$  (each year system will gain salt; eventually overturning will result simply by cooling).

understanding of the data themselves. Unfortunately, however, such an understanding is not readily available. Furthermore, the limited information provided by the weekly satellite images (mainly the presence or absence of sea-ice) is insufficient to provide a unique interpretation and the data thus lend themselves to subjective evaluation.

This subjectiveness is readily apparent in the interpretation of the short lived polynyas of 1973 (two) and 1977. Whether or not these periods of open water represent true polynyas, as discussed here, followed by a quick refreezing, or simply some local phenomena such as a storm-induced divergence of the ice, is difficult to ascertain from the satellite photos. Observations on the longitudinal migration of the polynya may shed some light on the interpretation of these short-lived events.

Fig. 10a contains the season-averaged polynya positions from 1973 to 1979, inclusive of these short-lived polynyas. Fig. 10b contains just their mean positions. As seen from these mean positions, there is some suggestion that the polynya is drifting westward at an average rate of  $\sim 0.01 \text{ m s}^{-1}$ . The direction and speed of polynya drift is similar to that of the expected wind-driven current of Gordon *et al.* (1981) and is significantly faster than the long Rossby

wave speed of  $\sim 5 \times 10^{-4} \text{ m s}^{-1}$ . For the years of their occurrence, the brief polynyas appear to be located in approximate agreement with the positions predicted for these respective years by this drift consideration. In light of this, although far from conclusive, we interpret these events as indeed, true (convective induced) polynyas, which in 1973 quickly refreeze.

A drift also would suggest other implications. For one, it is possible that such a drift would have an effect on the system. Fortunately, however, it is a simple matter to calculate the response of a system to a mass transfer between two layers in the presence of a mean shear flow (an extension of the problem considered by Gill *et al.* 1979). With the length scales relevant here it can be shown that the system will simply advect with the mean flow; the geostrophic adjustment (or "slumping" of the interface) taking place over a few kilometers only.

A further consequence of drifting also becomes apparent on examination of Fig. 10b. Here it is seen that sometime after the 1977 polynya ( $\sim 3-4$  years), the current would advect the preconditioned area into the western boundary current along the Antarctic Peninsula thus destroying and/or advecting the polynya out of the ice forming region. Furthermore,

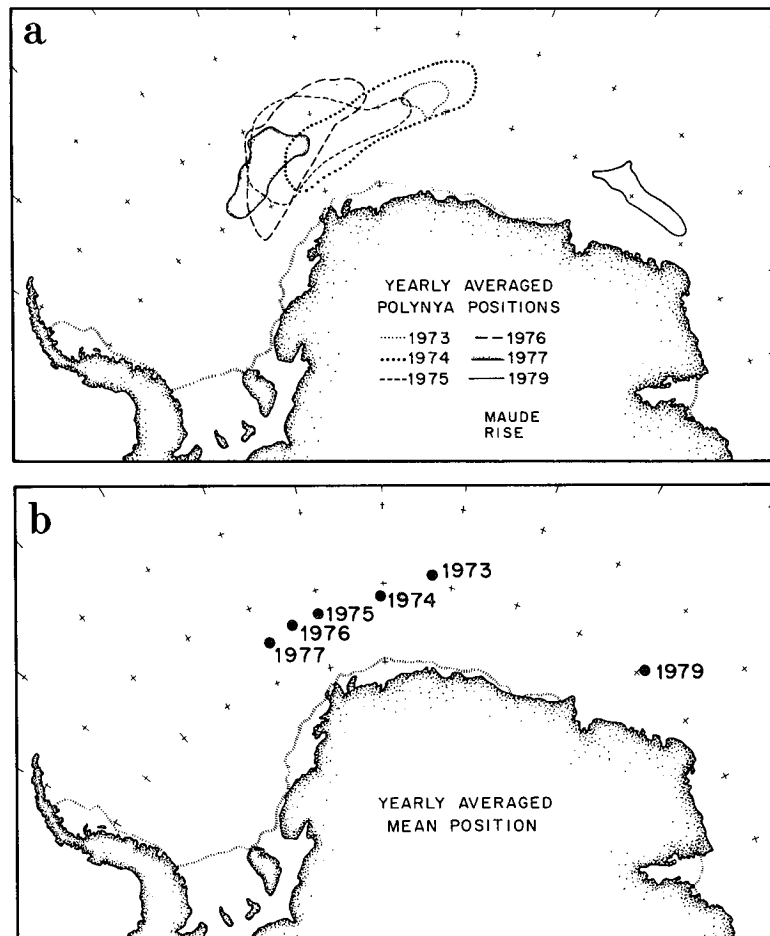


FIG. 10. Average polynya shape and position (a) for each year and mean position (b) of the polynya for each year.

a new polynya is seen to have formed in late September 1979, at  $\sim 40^\circ\text{E}$ . This anomalously eastern location may possibly suggest that as a result of further preconditioning, an overall cycle is beginning anew.

Because this latest polynya occurs  $\sim 32^\circ$  east of the 1973 position it could be interpreted (if one assumes an initial preconditioning at the approximate position of the 1979 polynya) as an indication that the 1973 polynya was already four or five years into a cycle (from the average drift rate of  $\sim 0.01 \text{ m s}^{-1}$ ) relative to its initial time of preconditioning. It then follows that a total cycle from preconditioning until destruction by advection might be as long as 12 years. Cycles which have or have not become stable (as described in Section 6c) are at this time destroyed in the western Weddell by northward advection.

Model results for just such cycles are presented in Fig. 11. The data also are presented in the figure to facilitate comparison, having been reduced to bar graph form which again involves interpretation. For

consistency, the following conventions were used. The time of ice formation in the area of the polynya is chosen as being the time in which a grid encompassing the average polynya (for the year in question in both size and position) is  $\sim 50\%$  covered by ice. This should eliminate any biases associated with earlier ice formation due to a more westward position of the polynya. The time chosen to represent the appearance of the polynya is that time in which an area of open water is first observed to be completely enclosed by ice.

Two cases have been presented, both utilizing parameter values within the ranges derived in the previous sections. We are obviously not compelled to assume that the preconditioning always occurs far to the east (there are no major topographic expressions at this location and it is south of the belt of maximum upwelling of Gordon *et al.*, 1977). For this reason case A represents the minimum limit in which the initial preconditioning of the cycle ending in 1978 was located at the position of the 1973 po-



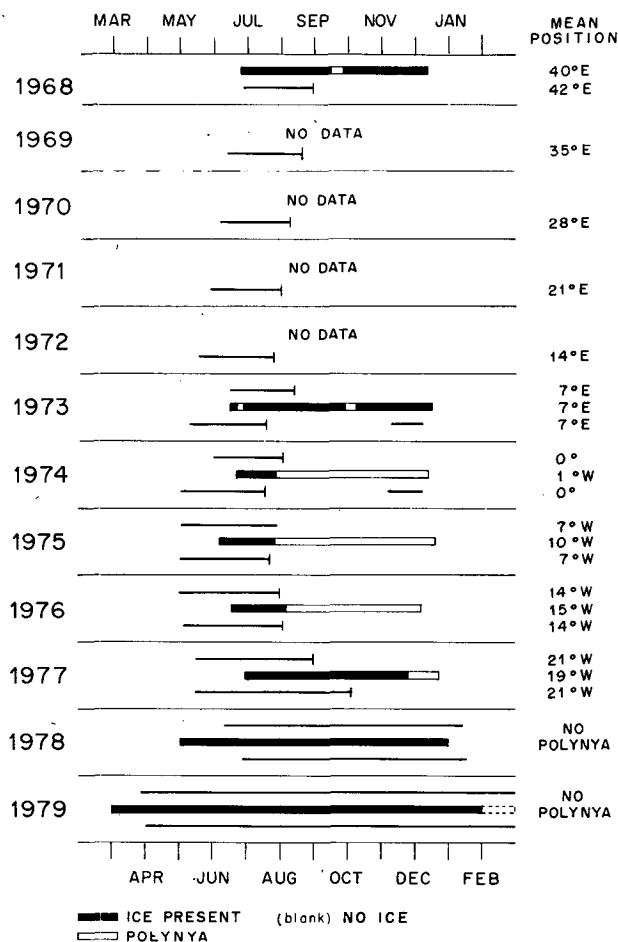


FIG. 11. Uppermost line for each year (starting in 1973) represents case A model results for  $F = 7.95\text{‰ cm day}^{-1}$  and  $S_1' = 34.46\text{‰}$  on 15 June 1973. Center line for each year represents data and the lower line, case B model results for  $F = 7.60\text{‰ cm day}^{-1}$  and  $S_1' = 34.46\text{‰}$  on 26 June 1968. Vertical bars on the model result ice-lines indicates overturn (followed by polynya). Data shown for 1968 are a replication of 1979,  $40^\circ\text{E}$  data and are for reference only (see text). Mean polynya positions, as predicted by the average drift rate, and actual mean positions are indicated, also.

lynya. Case B, however, represents model results consistent with the above suggestion of a  $40^\circ\text{E}$  position for the initiation of the cycle ending in 1978. The day of ice onset in the polynya area in 1968 is of course unknown. This time therefore has been tuned to yield the best overall cycle. Also, for comparison, we have replicated the 1979 eastern polynya as the 1968 condition. The position of the polynya center, as predicted by its average drift rate, also is shown for each year in Fig. 11 as are the actual observed positions.

In both cases the agreement between the model results and data is quite good. The timing of polynya formation is reproduced by the model both seasonally and yearly. Further, the ice distribution in the po-

lynya and non-polynya years are matched equally well, although ice onset appears to occur somewhat earlier in the model from 1974 to 1977. The non-polynya years depict the stable solution and case A therefore represents a 5-year cycle until stability, case B a 10-year cycle.

It is possible that the August 1979 ice degradation near the Antarctic Peninsula (Fig. 1) represents a final overturn event prior to destruction by advection. Both cases though, fail to reproduce such a polynya. This is not unexpected as the analyses of Section 6 indicate that once the cycle goes stable it will remain stable. It was stated, however, that the missing of a polynya prior to stability would be expected if state 4 were to be entered unusually late. This appears to be the case in 1977 followed by an exceptionally early ice onset in 1978 and 1979. An offset in timing from the model results such as this may be expected due to natural variations in the model parameters (examined in Section 8).

The values of  $F$  and  $S_1'$  for the model results are  $F \approx 7.95\text{‰ cm day}^{-1}$  (corresponding to a freshwater input of  $\sim 0.83\text{ m year}^{-1}$ ) and  $S_1' = 34.46\text{‰}$  for case A and  $F \approx 7.60\text{‰ cm day}^{-1}$  (corresponding to a freshwater input of  $\sim 0.79\text{ m year}^{-1}$ ) and  $S_1' = 34.46\text{‰}$  for case B, as expected, since  $F > F_{\text{crit}}$  in both of these cases, the system gains salt yearly and therefore requires more ice buildup each year before overcoming this extra salt and inducing overturn. Ice buildup in the model before overturning increased from 0.6 m to a maximum of  $\sim 1.1\text{ m}$ , averaging  $\sim 0.8\text{ m}$ . Consistent with the analyses of Section 6, the length of cycling was increased by decreasing  $|F - F_{\text{crit}}|$ .

Support for the values of  $F$  and  $S_1'$  in case A, in which we had control over the time of ice onset, is drawn by noting the results obtained by using actual station data for the initial conditions. Hydrographic stations 10 and 11 of Foster and Carmack (1976) are located at approximately  $25^\circ\text{W}$ ,  $65^\circ\text{S}$  and were taken around the first of February 1973. The location of these stations is at the same approximate latitude as the polynya and although they are  $25\text{--}30^\circ$  west of the 1973 polynya longitude, they might be expected to have similar  $T$  and  $S$  characteristics as they are located directly downcurrent of the actual polynya position.

A gross estimate of the average temperature and salinity of the water lying above the base of the pycnocline at these stations yields  $T \approx -1^\circ\text{C}$  and  $S_1' \approx 34.51\text{‰}$ . Assuming these to be the average characteristics, compressed into a 200 m deep upper level, in the preconditioned polynya area (as opposed to the  $\sim 300\text{ m}$  depth to the base of the pycnocline here, which is taken to correspond to the boundary between the upper and lower levels) the model was reevaluated. The results are nearly identical to those of case A for the same value of  $F$ . Except

for the onset of ice formation in the first year (1973), the other results agreed to within a week. The onset of ice formation in the first year, on the other hand, was 2 June, which is in fact close to the observed time ( $\sim 15$  May) of ice initiation in the vicinity of the stations where the actual data was collected. Overturning would not occur at the station locations, however, presumably due to the lack of preconditioning.

Although the manner in which these initial conditions were arrived at is far from ideal, it is interesting to note how their values induce nearly identical results to those obtained by using an entirely independent set of initial conditions, applicable nearly six months later in the year (in midwinter).

Alternative interpretations of the data are still feasible but require different model results. In particular, it may be interpreted that in the polynya years of 1974 to 1976, no ice whatever formed prior to the overturning event. This is entirely possible and corresponds to the state 1 condition of the model, in which the density of the upper level is such that overturn occurs simply as a result of cooling.

Model results consistent with this interpretation are presented in case A of Fig. 12. These results are obtained by reducing  $F$  such that its value is less than  $F_{crit}$ , as expected. As seen in the figure, for years prior to 1977 the model results again match the data (newly interpreted for 1974–76) quite well. Particularly impressive are the two polynyas obtained in 1973. However, as was indicated by the analyses of Section 6, once stability is obtained in the state 1 condition, the model, with constant  $F$ , is not capable of departing from this stability. The model results are therefore significantly different from the data for the years following 1976.

This does not imply that a state 1 condition is unacceptable. On the contrary, this interpretation of no ice forming in the polynya area prior to overturn is fully supported by the passive microwave images. These data seem to indicate that the ice forms around the polynya area, eventually closing it off completely but never actually forming in it (Claire Parkinson, personal communication).

Also, this interpretation is attractive from a consistency standpoint. As stated in Section 3, it might be expected that following an overturn induced by salt rejection during ice formation, the full 200 m thick upper level might not be reestablished immediately. Refreezing might then be expected to occur rather quickly due to the initially thin freshwater surface layer, unless heat is being continuously supplied from below. This refreezing is seen in the two polynyas of 1973 and the 1979 eastern polynya. It is hard to imagine then, why this is not seen in 1974–76, unless, either the physics has changed or, indeed, there is a continuous supply of heat from below (i.e., our state 1 condition). This, combined with the fact that the full season polynyas

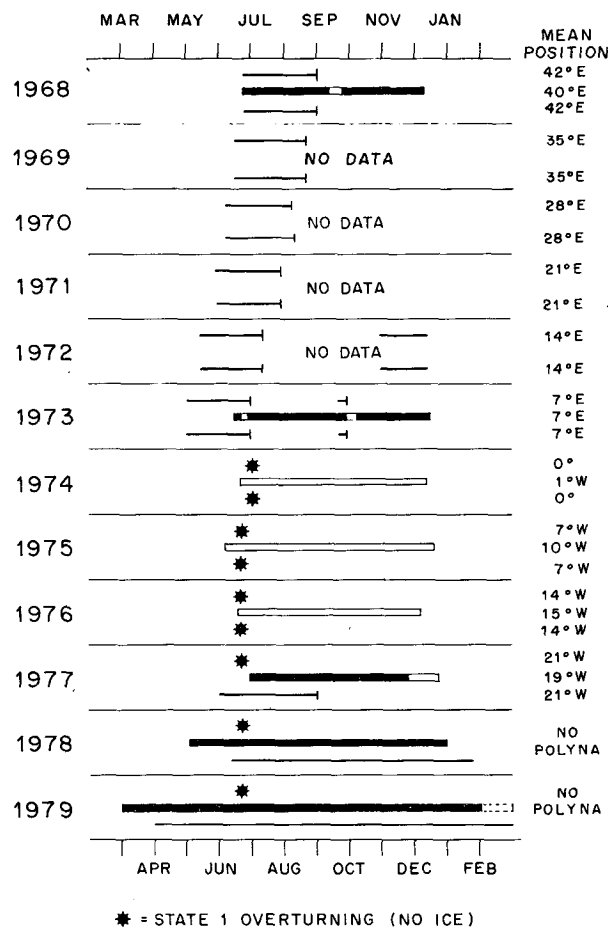


FIG. 12. Case A model results (uppermost line) for  $F = 7.48\%$  cm day $^{-1}$  and  $S_1' = 34.46\text{‰}$  on 24 June 1968 inducing a permanent state 1 stability by 1974. Data (center line) represent alternative interpretation for the 1974–76 sea-ice distribution in the polynya area. Case B model results (lowermost line) uses same  $F$  and  $S_1'$  values as case A but in 1976 polynya area receives 0.86 m of freshwater input from in-drifting sea-ice which destabilizes the state 1 condition. Interpretations and mean positions for model and data are as in Fig. 11.

of 1974–76 are the *only* ones which possibly occur without prior ice formation seems to be consistent with a state 1 stability starting in 1974.

Further, the model has been run numerous times under varying conditions and with different parameter restrictions and values (described in Section 8). Under all conditions, in the year prior to a state 1 stability, if a polynya occurs in late June/early July, as one did in 1973, it was invariably followed by a refreezing and second polynya formation in late September/early October, again as observed in 1973. This then, is also consistent with a state 1 interpretation of the 1974–76 data. In the model, under all conditions the occurrence of two polynyas in a single year is always followed by a state 1 stability the next year.

If this interpretation is indeed correct, how then might this stable state 1 condition be destabilized? Several possibilities exist. For example, the decay or degradation of the preconditioning with time, or as the area drifts westward may be sufficient to destroy the stability. A large input of fresh water from sea-ice drifting into the polynya area and melting also may serve to shock the system into another state. As roughly derived in Section 5, it was shown that we might expect as much as 0.86 m of freshwater input as a result of in-drifting sea-ice. If this freshwater input does not exceed 0.65 m (beyond its normal contribution to  $F$ ) the state 1 condition can not be destabilized. For larger values though, destabilization does take place and any pattern of cycling can be made to follow. That pattern which best matches the data is attained by an anomalous input of 0.86 m (the derived maximum amount available) into the polynya in 1976. Results for this case are shown in Fig. 12, case B. As seen, these results now match the data quite well for all years.<sup>6</sup>

This interpretation can therefore be matched by the model equally well, simply by relaxing the constant  $F$  assumption. Whichever interpretation is correct, however, will only be discernable by closer observation. Regardless of the interpretation, it would appear that the model can, at this stage, accurately simulate most of the data both temporally and spatially in spite of the overall cycle length, while utilizing the physically realistic values previously established for the model parameters.

## 8. Sensitivity of the model

### a. Stochastic forcing in $Q$ and $F$

The results of the model reproduce the observable features of the data, essentially by tuning the free parameter  $F$  at a particular value of  $S_1'$ . It might be argued of course that irregularities in the data are caused not by cycling within the system, but more simply by variations in the surface heat flux or net precipitation from day to day, month to month, etc. To test this, the model was subjected to a variety of stochastic variations in the parameters  $Q$  and  $F$ , which were thought to best simulate the variations expected in nature. These tests were conducted using the case A model results of Fig. 11, as a basis and include the following:

<sup>6</sup> As frequently occurs in physical modeling, a model tending to stability indicates that some higher order physics may be missing which would provide a feedback mechanism preventing the stability. Lateral (or other) effects may provide that mechanism in this case. The 0.86 m of fresh water quoted here to "shock" the system out of stability may indeed represent some more gradual or combination of lateral or feedback effects not considered by this simple, first order model. While effects such as these would likely alter the timing of the overturn events, especially as we approach stability, they would not invalidate our major findings.

(i)  $Q_i$  and  $Q_w$  were varied daily, monthly, seasonally and yearly by as much as  $\pm 20\%$  on a random basis.

(ii)  $F$  was also varied stochastically over these same time scales by  $\pm 20\%$ .

(iii) Finally, various combinations of (i) and (ii) were tested.

Each test was repeated a total of nine times using a different random sequence. The results of the tests in the variation of the heat flux were similar to those of the daily variations in all of the tests. Minor effects occurred. The timing of overturn, ice onset, etc., varied by a week or two over a period of six years from the unperturbed calculations. Of course, over a period of one month one would assume  $\int Q \approx \int \hat{Q}$  and  $\int F \approx \int \hat{F}$  so these results for the daily variations are not unexpected.

Tests involving variations in  $F$  (including those with  $Q$ ) on a monthly basis, for the most part, produced slight change or induced stability a year earlier or later than the unperturbed results (similar results were obtained by varying  $F$  as much as 50% daily). On a seasonal or yearly basis, however, the results were more pronounced. In these tests, clearly 50% of the time, the system became stable (in a state 1 condition) within three years. Results for the other 50% were like those for the monthly variations.

From these tests it is seen that natural variations in the heat flux as well as day-to-day variations in the net precipitation should have little effect in the overall pattern of cycling observed. Longer term variations in net precipitation though, may have effects in both the timing of the stability and more significantly, in the type of stability obtained. Although this obviously creates an uncertainty in the actual values assigned to  $F$  in Section 7, for a particular interpretation of the data, it does show that a natural variation in meteorological parameters is not required to provide irregularities in the system response (i.e., the basic analyses of Section 6 still hold, and simple variations in these parameters will not produce an independent cycling).

### b. Effects of preconditioning

The sole parameter whose variation has not yet been discussed is the upper level depth  $h$ , which is arguably fixed by observations. However, since the polynya area is clearly anomalous, it is of interest to see what happens to the ice cycle in regions of greater or smaller pycnocline depth.

From Eqs. (6.2) and (6.4) it is seen that the value of  $h$  effects only the time scale of the processes and not the slopes in  $T-S$  space. Therefore at a specific value of  $F$ , a doubling of  $h$  would require twice as much time until freezing or overturning. A halving of  $h$ , on the other hand, would produce just the opposite effect. From this it is seen that the overall

effect of an increase in  $h$  is to decrease the likelihood of overturning whereas a decrease in  $h$  would increase the likelihood.

The model has been tested for changes in  $h$ , again, using case A results as a basis. The testing indicates that for  $200 \text{ m} \leq h \leq 225 \text{ m}$  the results are similar to the unperturbed case with slight differences arising only in the timings of ice onset and overturning by at most two weeks. For  $h \geq 225 \text{ m}$  the system becomes stable progressively earlier; by  $300 \text{ m}$  overturning occurs late in year one only and for  $h \geq 340 \text{ m}$  the system is permanently stable (full ice cover in the cooling seasons). For shallow  $h$ , stability occurs quickly and with  $h \leq 175 \text{ m}$  the system has gone stable by year 2 (overturn induced by cooling).

It is possible though, to generate acceptable cycles for a range of  $h$  values by adjusting the main parameters  $F$  and  $S_1'$ . For shallow  $h$  values the system becomes very sensitive and to maintain a cycling, a much narrower range of  $F$  and  $S_1'$  is required. With  $h = 100 \text{ m}$ , at best a five year cycle was produced using  $F = 7.8\% \text{ cm day}^{-1}$  and  $S_1' = 34.44\%$ . For deeper  $h$  values the system becomes sluggish and requires a higher input of fresh water to balance the overturn. Values of  $h \geq 275 \text{ m}$  require values of  $F \geq 9.5\% \text{ cm day}^{-1}$  to maintain even a six year cycle. Longer cycles require prohibitively larger values of  $F$ . From these results it is possible to conclude that, in general, the  $200 \text{ m}$  depth chosen for the model and supported by observation appears to be near the center of an  $\sim 100 \text{ m}$  range in depth ( $\sim 150\text{--}250 \text{ m}$ ), in which the observed cycling patterns can be produced. Shallower values of  $h$  cannot be ruled out though as they are more easily shocked out of state 1 and with a variable  $F$  are quite susceptible to irregular, long-term cycling.

### c. Miscellaneous testing

Variations in  $K$  were examined, again, using case A results as a basis. The parameter was decreased by a factor of 5 with negligible effect on the results. Decreased by an order of magnitude, it prolonged the period of ice melting following overturn and slightly altered the time scale of the ice onset and overturning. The exact value of  $K$  therefore is considered noncritical in the cycling observed.

Finally, the model was run under various conditions and assumptions which differ from those originally used. These variations included the following:

- 1) The freshwater input  $F$ , was added as snow, at  $-20^\circ\text{C}$ , for the entire year, each year. This was accomplished by adding the term  $-FL_w/\sigma C_p$ , where  $L_w = 418.4 \text{ J g}^{-1}$ , to (3.1a) and (3.2a).

- 2) The freshwater input  $F$ , was added as rain for the entire year each year. It was then released as an accumulated freshwater sum  $F_a = \int dF/dt$  after ice melt.

- 3) An entirely different set of heat flux values was used which contained monthly values  $\sim 15\%$  higher than the set presented in Table 1.

- 4) Various combinations of the main parameters (i.e.,  $F$ ,  $K$ ,  $K_T$ ,  $K_S$  and  $h$ ) were altered; usually including an extreme value for one of the parameters.

In each of these first three cases, model results nearly identical to those presented in Figs. 11 and 12 were attained by slight adjustments in the value of  $F$  and  $S_1'$ . The largest change to  $F$  was required when using the heat flux values of 3). In this case  $F$  was increased  $\sim 12\%$  before attaining similar results. In the other tests  $F$  was changed only a couple percent at most. In case 4 both regular and irregular cycling patterns were consistently attained by working within acceptable ranges for the varied parameters excluding the extreme value. For example,  $K_T$  and  $K_S$  were increased by an order of magnitude yet cycling patterns were attained using values of  $F$  within our derived range and changing  $h$  no more than  $100 \text{ m}$ . We feel that when these tests are combined with the tests described earlier in this section, the overall success of the model under such a variety of conditions and parameter values adds considerably to its credibility.

## 9. Speculations and discussion

A discussion along with several testable, qualitative predictions resulting from this study, can now be stated.

First, the polynya can be expected to contribute a large proportion to the deep water formation around Antarctica. If only  $200 \text{ m}$  of surface water contributes an area of  $0.3 \times 10^6 \text{ km}^2$  of deep water every other year, the (lower) limit obtained is  $10^6 \text{ m}^3 \text{ s}^{-1}$ . This deep water would be  $\sim 0.1^\circ\text{C}$  colder and  $\sim 0.01\%$  fresher than the surrounding warm deep water.

Such a signal has been observed by Gordon (1978) near his critical  $\sigma_2$  value of  $\sim 37.22$ . Furthermore, one of the authors (ALG) is currently comparing the 1973 deep-water temperatures west of Maud Rise (before the polynya occurred in this region) with the 1978 summer data in the same area (after the three large polynyas occurred). In direct agreement with what this theory predicts he has found a cooling of the deep water ( $\sim 0.3^\circ\text{C}$  cooler) in the post polynya years. This water covers an area  $\sim 4$  times the size of the polynya which is consistent with an excess sea-air heat flux in the polynya of  $\sim 240 \text{ W m}^{-2}$ ; about the value expected for open ocean in the winter. The magnitude of these values therefore add further support to the theory.

Second, it is suggested that the polynya might form somewhere in the south eastern or central portion of the Weddell subpolar gyre and drift slowly westward, averaging  $\sim 7^\circ \text{ year}^{-1}$  (slower in the east, quicker in

the west). Fortunately, the extreme eastern nature of the 1979 polynya should provide an excellent basis from which to test this idea over the next few years. Also, years with small, short-lived polynyas, (lasting less than two weeks to a month before refreezing) may eventually give way to years with large polynyas lasting the entire ice season. These may be preceded by the occurrence of two, short-lived polynyas the prior year, or by the formation of the polynya due to ice forming completely *around* (not in) the polynya area. These large polynyas themselves may then give way to another cycling pattern following a season in which an abnormally large amount of sea-ice drifts into the polynya and melts. The model suggests that when the polynya does appear, the ocean surface layer temperature and salinity should not be too far from the deep water values and the temperature should certainly be well above freezing. Indeed, during the large, full ice season polynyas, there should be no distinct surface layer at all.

Finally, we have thus far ignored the effects of topography on the polynya area and what effect it might have on the preconditioning. Enhanced Ekman bottom pumping is to be expected over regions of strong topography and this could strongly modify the dynamics of the system due to an extra vertical mass transfer. Maud Rise, for example, located at 65°S, 0°E (Fig. 10a), reaches to within 1000 m of the surface and Gordon's (1978) maps show a large thermal and saline disturbance there. Furthermore, Fig. 10a shows that the polynya, while drifting westward, does seem to be slowed down near Maud Rise. Could, perhaps, such a topographical feature "capture" the polynya for a time?

It is difficult to answer this question at this time, but we can attempt an estimate. From a geostrophic balance we might expect horizontal velocities in the polynya to be of order  $0.2 \text{ m s}^{-1}$  near-surface. These are strongly baroclinic however, and near-bottom velocities would (if following a vertical modal structure) be of order  $hH^{-1}$  less, or  $\sim 0.01\text{--}0.02 \text{ m s}^{-1}$  which is the order of the mean barotropic flow in the area. Assuming that vorticity balance induces a doubling of horizontal velocities over strong topography, the usual quadratic drag law on the bottom yields an Ekman pumping of order  $6 \times 10^{-7} \text{ m s}^{-1}$ , which is about the value of  $K_T$  used anyway. Only if bottom velocities were of the same order as the surface velocities could we expect a strong modification of the system by Ekman pumping. This would involve a circulation in the polynya of  $60 \times 10^6 \text{ m}^3 \text{ s}^{-1}$  or more, which, though possible, seems unlikely. Therefore, topography may have a role to play in the dynamics of the polynya, but further analysis is necessary to prove this.<sup>7</sup>

There also are points which mitigate against any topographical effects directly producing a preconditioning effect. The first is that the areal extent of the polynya is much larger than any relevant topographic feature. The second is the observation that the 1979 polynya was initiated in an area far east (40°E) of Maud Rise, in a region of no noticeable topography, although this location may turn out to be anomalous.

What other form might the preconditioning take then? A long-lived cyclone could possess approximately the correct length scales for preconditioning, but to move an isopycnal 100 m vertically in, say, one month would require a  $w$  of  $3.8 \times 10^{-5} \text{ m s}^{-1}$ , a very high value. For this, a steady wind stress of  $5 \text{ N m}^{-2}$  would be needed which is at best unlikely.

We are thus led to consider whether the mean flow itself might be capable of preconditioning the polynya area (as distinct from participating in the polynya dynamics during the process). The response to a cyclonic wind system, by an ocean initially at rest, is a uniform raising of isopycnals in the ocean interior (a "spinning up") until the influence of the oceanic boundaries is felt in the form of Rossby waves (Anderson and Gill, 1975). For our purposes we need only consider the baroclinic Rossby waves, which are relatively unaffected by topography (Anderson and Killworth, 1977). Such a spin-up would require 6–10 years to raise isopycnals by 100 m. Since the Rossby waves are so slow in this area, these will not have a significant effect on the spin-up over this time scale.

We might thus imagine the following sequence of events. As spin-up takes place, the thermocline gradually domes upward in the Weddell gyre. The center of the dome would reach 200 m before the rest of the gyre (unless the pre-existing mean flow, which the arguments about preconditioning and Rossby waves have ignored, could modify this response). There might thus be a polynya for one season but the continued raising of the thermocline would tend to move the polynya area to the north and south of the gyre center. To the north, the freezing rate becomes less and the polynya disappears. In the south, however, a cycle of the form we have discussed takes place. This modifies the circulation in the vicinity of the polynya (which tends to be around the polynya, not across it). The area advects westward with the mean flow towards its ultimate destruction. If we assume a "filling-in" of water from outside the gyre or a "return-to-normal", we would anticipate a region of flatter isopycnals left behind the polynya. If this is so, over the next years the original polynya area would spin up again and at some later date the process would reinitiate.

Lacking wintertime hydrographic data, we must stress that the above discussion is speculation, and

<sup>7</sup> We are indebted to a referee for a discussion on this point.

likely to remain so for some time to come. However, the appearance of the September 1979 polynya at 40°E may indeed confirm this and it will be interesting to note over the next few years if the polynya appears to be drifting west from this position.<sup>8</sup>

## 10. Conclusion

We have proposed a simple, one-dimensional model which seems to contain the basic physics required to simulate the polynya situation. The model has performed well in testing our initial theory despite its simplicity and limitations in regard to attaining the parameter values. It has been tested and shown to be successful under a broad range of conditions and parameter values and thus warrants further development (e.g., the inclusion of lateral effects, higher order physics, etc.). It would also appear that at this stage the model can offer first-order answers to the three questions originally addressed. These are as follows:

1) The polynya seems to result from haline-induced vertical convection due to salt rejection, by the freezing of sea-ice, into a preconditioned upper level. This brings up enough heat from the warm deep water below to melt the ice far earlier than the seasonal surface heat flux would itself permit.

2) The polynya's occurrence is irregular because of the sensitive nature of its time scale on the various  $T - S$  characteristic slopes, and on the freshwater input. Some natural variations in the surface heat flux and freshwater input also may play a role. Further, eventual stability and/or a westward drift of the polynya from some initial preconditioning area, would cause the ultimate destruction of any one particular cycle. The nature of each cycle pattern might therefore be expected to depend on the salinity and temperature characteristics of the surface level water mass, above the pycnocline, in the area of preconditioning as well as on the amount of fresh water entering the system each year.

3) Finally, the polynya appears to occur in the belt in which it has been observed due to a preconditioning which is responsible for compressing the surface layer above the pycnocline into a shallow layer of ~150–250 m thickness. It is at this thickness that the system appears to be most susceptible to overturning for the amount of fresh water entering the system. Distribution of the polynya over the belt

may then be due to either the broad nature of this preconditioning or to a drifting of the preconditioned area with the mean current.

*Acknowledgments.* This work originated while the authors participated in the 1979 Woods Hole Oceanographic Institute, Geophysical Fluid Dynamics Summer Study Program. We thank all the other participants and staff, especially Drs. Melvin Stern and George Veronis, for their hospitality, advice and skepticism. Thanks also go to Dr. Claire Parkinson for her help with the microwave satellite data. Support for D.G.M. and A.L.G. at Lamont-Doherty was through National Science Foundation Grant DPP-78-24832. Support for P.D.K. at Cambridge was by a grant from the Natural Environment Research Council of Great Britain.

## REFERENCES

- Anderson, D. L. T., and A. E. Gill, 1975: Spin-up of a stratified ocean, with application to upwelling. *Deep-Sea Res.*, **22**, 583–596.
- , and P. D. Killworth, 1977: Spin-up of a stratified ocean, with topography. *Deep-Sea Res.*, **26**, 709–732.
- Bryan, K., 1969: A numerical method for the study of the circulation of the world ocean. *J. Comput. Phys.*, **4**, 347–376.
- Carsey, F., 1980: Microwave observations of the Weddell polynya. *Mon. Wea. Rev.*, **108**, 2032–2044.
- Fleet Weather Facility (FLEWEAFAC): 1973–1979: Weekly ice charts, Southern Hemisphere (northern ice limit). U.S. Dept. of the Navy.
- Fletcher, J. O., 1969: Ice extent on the Southern Ocean and its relation to world climate. Memo. RM-5793-NSF, The Rand Corp., Santa Monica, CA, 108 pp.
- Foster, T. D., and E. C. Carmack, 1976: Temperature and salinity structure in the Weddell Sea. *J. Phys. Oceanogr.*, **6**, 36–44.
- Gill, A. E., J. M. Smith, R. P. Cleaver, R. Hide and P. R. Jones, 1979: The vortex created by mass transfer between layers of a rotating fluid. *Geophys. Astrophys. Fluid Dyn.*, **12**, 195–220.
- Gordon, A. L., 1978: Deep Antarctic convection west of Maud Rise. *J. Phys. Oceanogr.*, **8**, 600–612.
- , 1981: Seasonality of southern ocean sea ice. *J. Geophys. Res.* (in press).
- , and E. Molinelli, 1981: *Southern Ocean Atlas: Thermohaline and Chemical Distributions*. Columbia University Press (in press).
- , and T. Baker, 1981: *Southern Ocean Atlas: Objective Analysis*. Columbia University Press (in press).
- , H. W. Taylor and D. T. Georgi, 1977: Antarctic oceanographic zonation. *Polar Oceans—Proceedings of Polar Oceans Conference May 1974, Montreal Canada*, M. J. Dunbar, Ed., Arctic Institute of North America, 45–76.
- , D. G. Martinson and H. W. Taylor, 1981: The wind-driven circulation in the Weddell-Enderby Basin. *Deep-Sea Res.*, **28**, 151–163.
- James, R. W., 1966: Ocean thermal structure forecasting. *ASWEPs Manual*, Vol. 5, SP105, U.S. Naval Oceanographic Office, 217 pp.
- Heap, J. A., 1964: Pack ice. *Antarctic Research*, R. Priestley, R. J. Adie and G. De Q Robin, Eds. Butterworth, 360 pp.
- Killworth, P. D., 1976: The mixing and spreading phases of MEDOC. I. *Progress in Oceanography*, Vol. 7, Pergamon Press, 59–90.
- , 1979: On “chimney” formations in the ocean. *J. Phys. Oceanogr.*, **9**, 531–554.

<sup>8</sup> Since the original submission of this paper, a short-lived polynya appeared again (in July, 1980) at ~40°E. This seems to reaffirm that the cycling is beginning anew in the east. Also, although it has shown essentially no westward drift relative to the 1979 position it is not inconsistent with the drift hypothesis. Indeed, at this eastern position of the Weddell subpolar gyre the drift rate is extremely slow and several years may be required before it is caught into the main flow.

- Lemke, P., 1979: A model for the seasonal variation of the mixed layer in the Arctic Ocean. *Lectures from the 1979 Summer Study Program in Geophysical Fluid Dynamics at the Woods Hole Oceanographic Institution*, Vol. II, WHOI Ref. 79-84, 82-96.
- Loewe, F., 1967: Antarctic meteorology. *Encyclopedia of Atmospheric Sciences and Astrogeology*, R. W. Fairbridge, Ed., Reinhold, 19-27.
- Moritz, R. E., 1979: Penetrative convection behind a moving, horizontal temperature discontinuity. *Lectures from the 1979 Summer Study Program in Geophysical Fluid Dynamics at the Woods Hole Oceanographic Institution*, Vol. II, WHOI Ref. 79-84, 29-62.
- Newton, C. W., 1972: Southern Hemisphere general circulation in relation to global energy and momentum balance requirements. *Meteorology of the Southern Hemisphere*, C. W. Newton, Ed., *Meteor. Monogr.*, No. 35, Amer. Meteor. Soc., 215-246.
- Streten, N. A., 1973: Satellite observations of the summer decay of the Antarctic sea-ice. *Arch. Meteor. Geophys. Bioklim.*, A22, 119-134.
- Turner, J. S., 1973: *Buoyancy Effects in Fluids*. Cambridge University Press, 367 pp.
- van Loon, H., 1972: Cloudiness and precipitation in the Southern Hemisphere. *Meteorology of the Southern Hemisphere*, C. W. Newton, Ed., *Meteor. Monogr.*, No. 35, Amer. Meteor. Soc.
- Voorhis, A., and D. C. Webb, 1970: Large vertical currents observed in a western sinking region of the northwestern Mediterranean. *Cah. Océanogr.*, 22, 571-580.
- Vowinckel, E., and S. Orvig, 1970: The climate of the North Polar Basin. *World Survey of Climatology*, Vol. 14, *Climate of the Polar Regions*, S. Orvig, Ed., Elsevier, 379 pp.
- Welander, P., 1977: Thermal oscillations in a fluid heated from below and cooled to freezing from above. *Dyn. Atmos. Oceans*, 1, 215-223.
- Wüst, G., W. Brogmus and Die Zonal Verteilung von Salzgehalt, 1954: Temperatur und Dichte an der Oberfläche der Ozeane. *Kiel. Meeresforsch.*, 10, 137-161.